ASSESSMENT OF SHAPE MEMORY ALLOYS – FROM ATOMS TO ACTUATORS – VIA *IN SITU* NEUTRON DIFFRACTION

Othmane Benafan

Structures and Materials Division

NASA Glenn Research Center

Cleveland, OH 44135

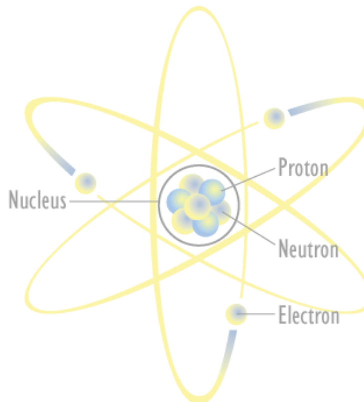

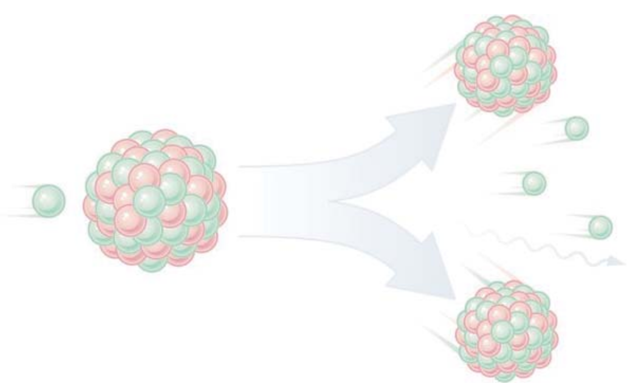

The ASME 2014 Conference on Smart Materials, Adaptive Structures and Intelligent Systems, September 8-10, 2014 – Newport, Rhode Island

It Takes a TEAM …

S.A. Padula II, R.D. Noebe, A. Garg, D.J. Gaydosh, G.S. Bigelow and T.J. Halsmer

Structures and Materials Division

NASA Glenn Research Center

R. Vaidyanathan and D. E. Nicholson

Advanced Materials Processing and Analysis Center

Materials Science and Engineering Department

University of Central Florida

B. Clausen and D. Brown

Los Alamos Neutron Science Center

Los Alamos National Laboratory

K. An and H.D. Skorpenske

Spallation Neutron Source

Oak Ridge National Laboratory

Acknowledgment

- NASA Fundamental Aeronautics Program, Fixed-Wing and Aeronautical Sciences Projects
- Basic Energy Sciences (DOE)

Motivation and Objectives

- We examine microstructures of:
  - Conventional structural materials by quenching in the high temperature structure and examining at room temperature.
  - This cannot be done for SMA’s because of the diffusionless phase transformation (austenite/martensite) cannot be suppressed by quenching

Length Scale in Engineering Materials
Where Does Neutron Diffraction Fit?

ATOMIC SCALE
(NANOMATERIALS)

MICRO-SCALE
(MICROSTRUCTURES)

STRUCTURAL SCALE
(COMPONENTS)

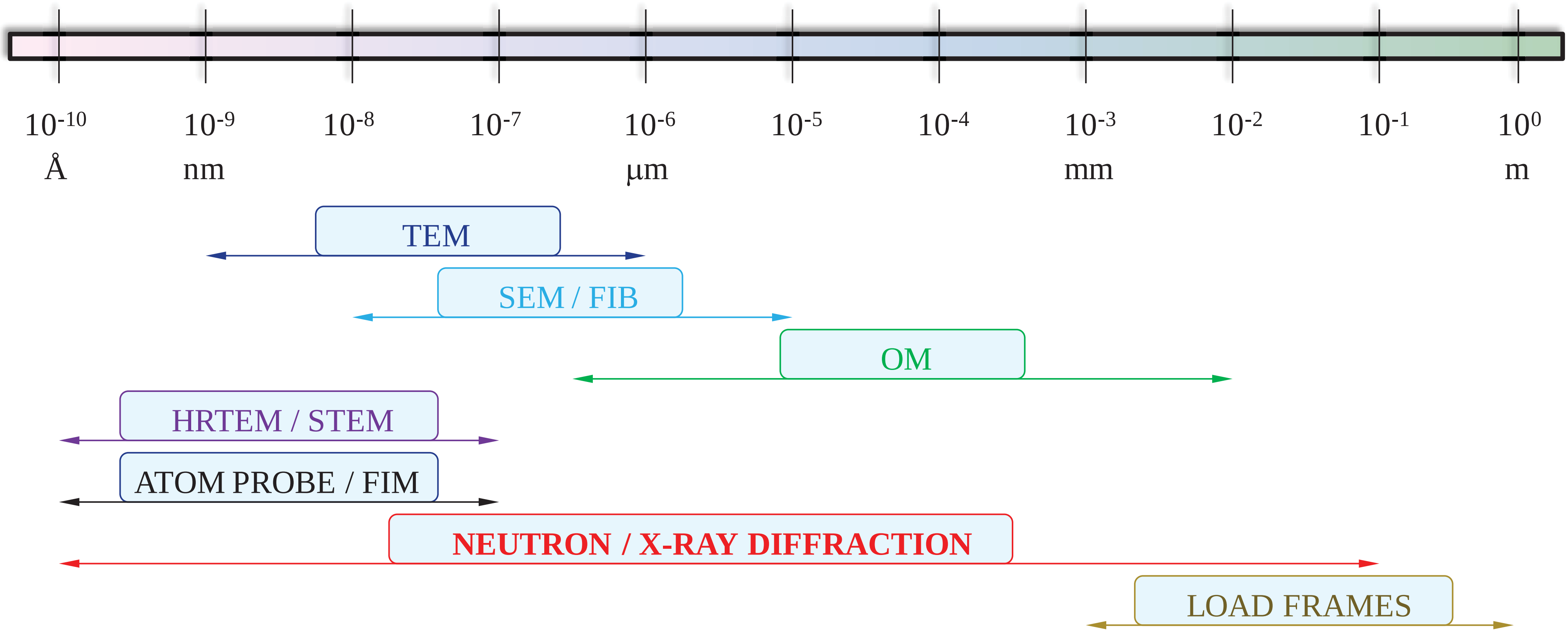

Applications of Neutron Diffraction

Chemistry

Physics

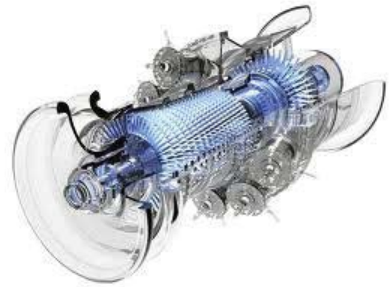

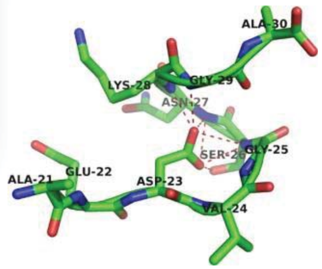

Engineering

Life sciences

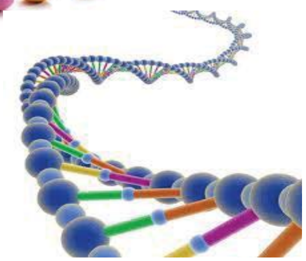

Biosciences

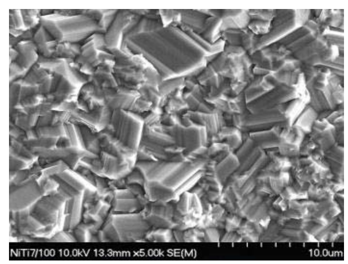

Materials science

Geological sciences

Archeology

W. Kockelmanna et al.

Courtesy: Mario Bieringer

Neutrons at the Experimental Area

- **Now we have neutrons, what next?**

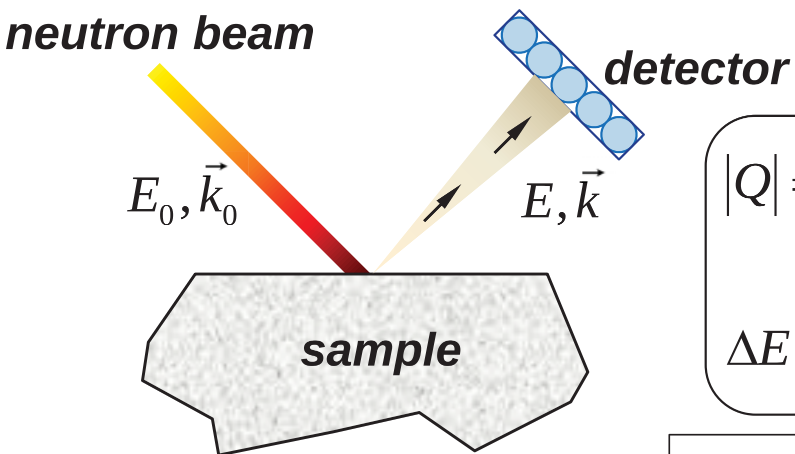

$$|Q| = |\vec{k}_0 - \vec{k}| = \frac{4\pi \sin\theta}{\lambda}$$

$$\Delta E = E_0 - E = \hbar\omega = \hbar^2 \frac{\left(k_0^2 - k^2\right)}{2m}$$

Nomenclature

k: wavevector
E: energy
Q: scattering vector
ħ: reduced Planck constant
m: mass (1.67 x 10^{-24}g)
λ: wavelength
2θ: scattering angle

- Neutron beam with a known wavevector (k_0) and energy (E_0)
- Detect number of scattered neutrons with a wavevector (k) as a function of the scattering function $S(Q,\omega)$

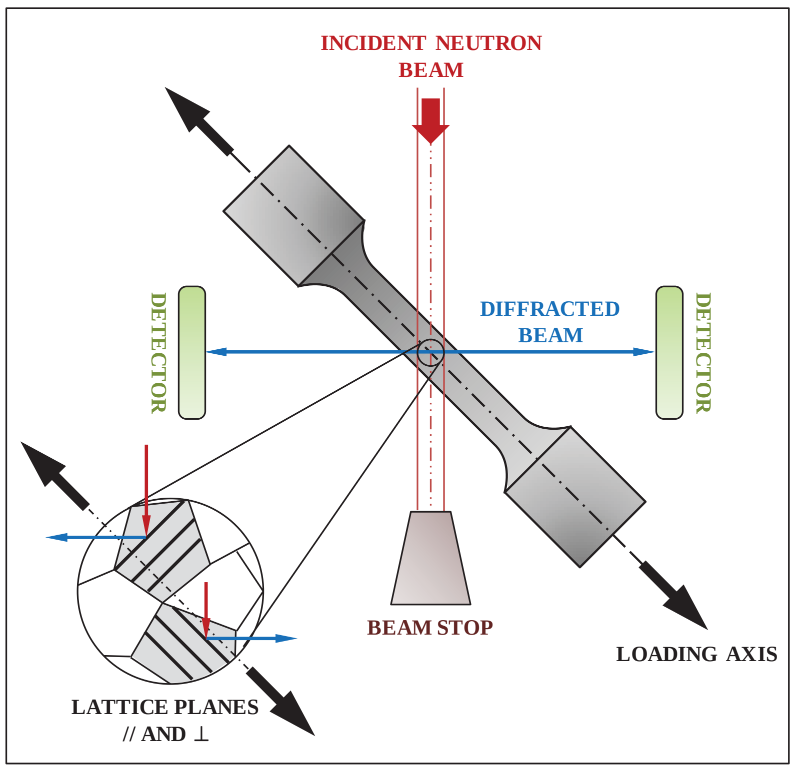

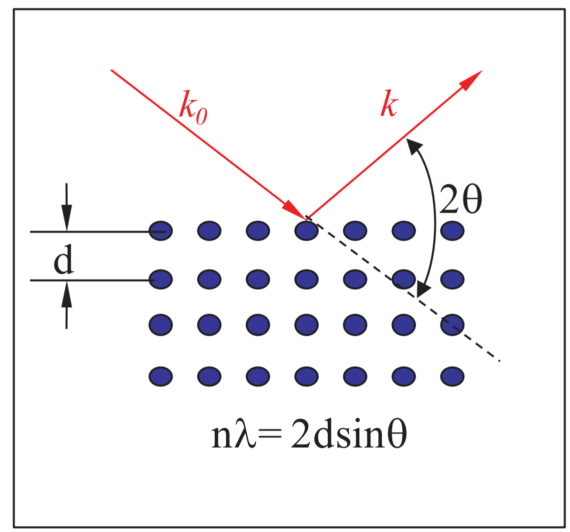

Neutron Diffraction Data

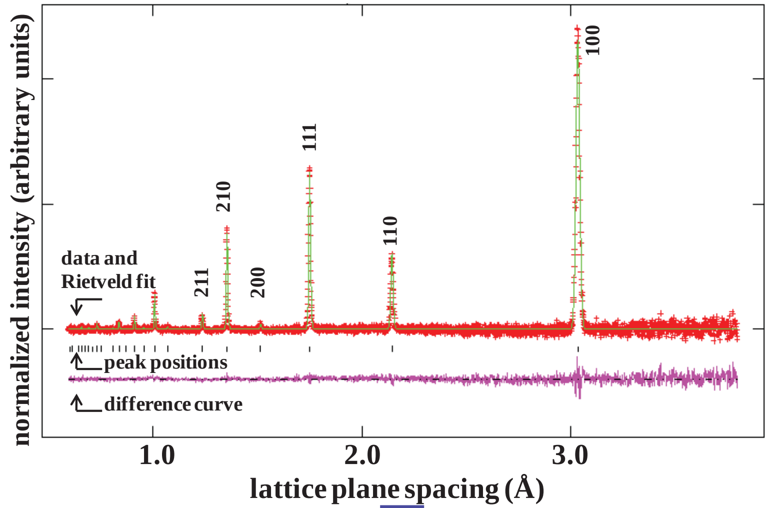

- **Peak position**
  - •Elastic lattice strain
  - •Intergranular strains

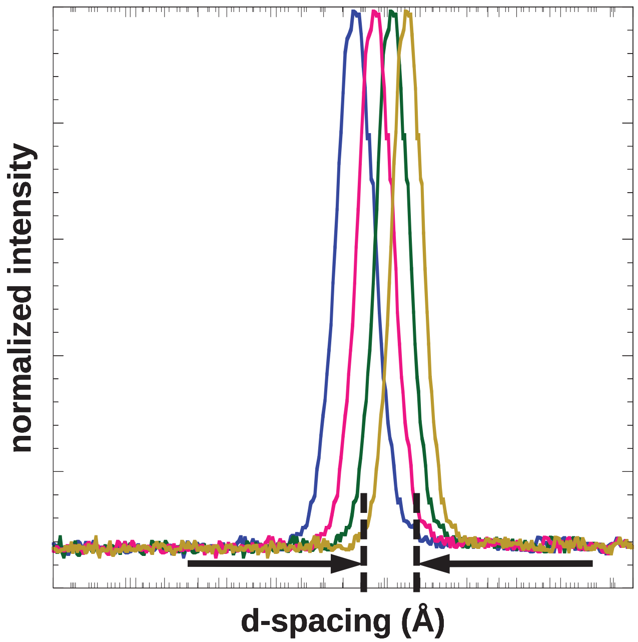

- **Peak intensity**
  - •Texture changes
  - •Phase fraction

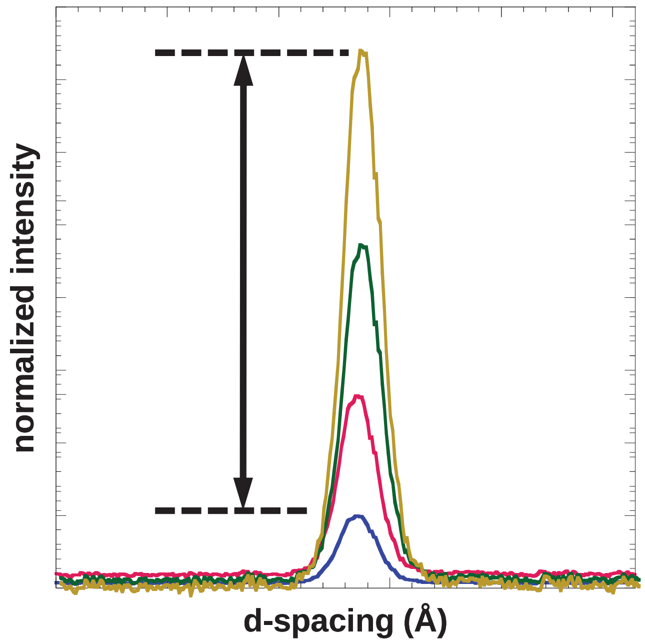

- **Peak width**
  - •Qualitative information

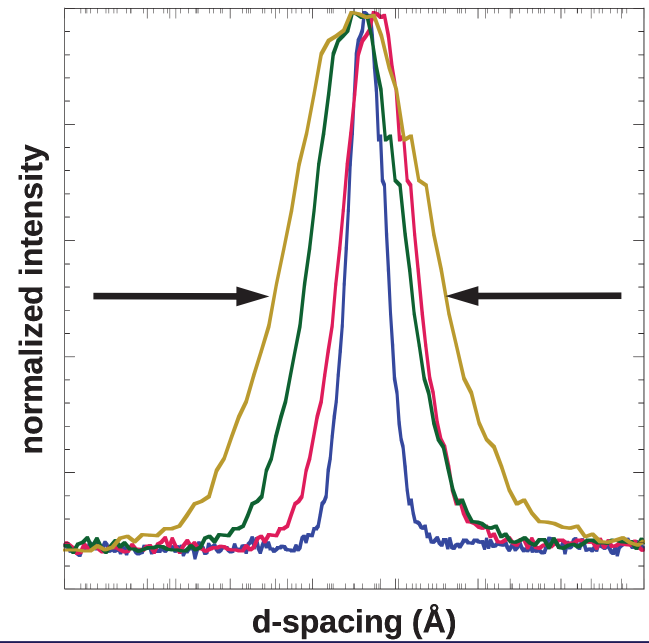

Neutron/Synchrotron Sources in the USA

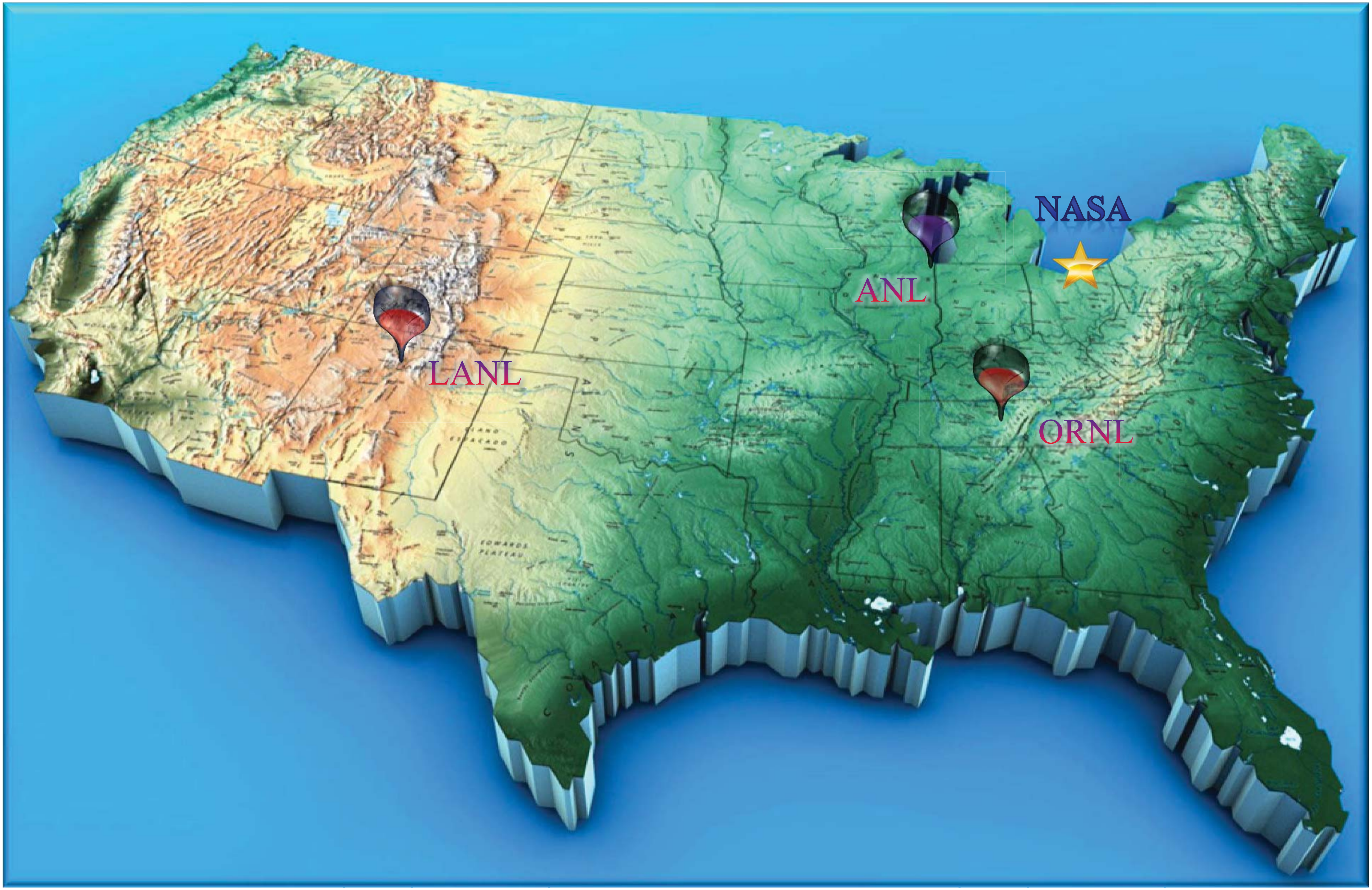

Neutron and Synchrotron Sources Around the World

Oak Ridge National Laboratories-SNS

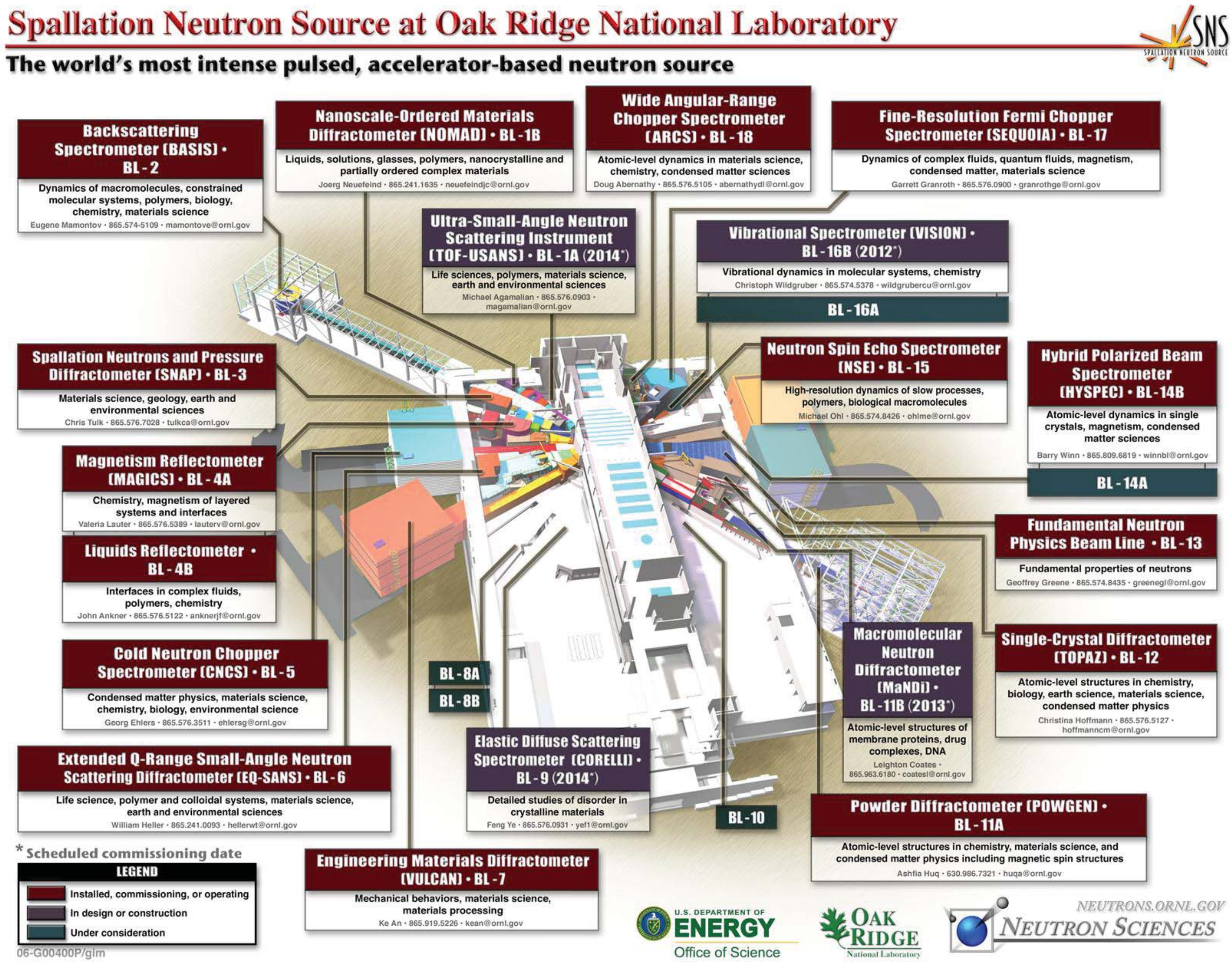

Los Alamos National Laboratory-LANSCE

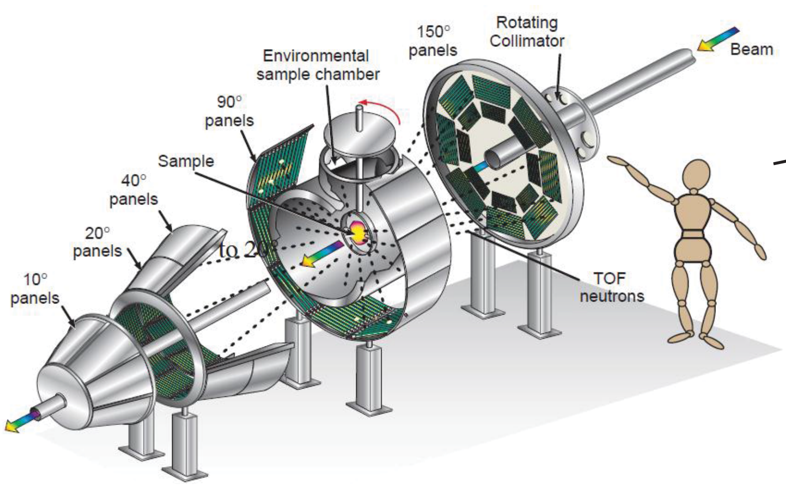

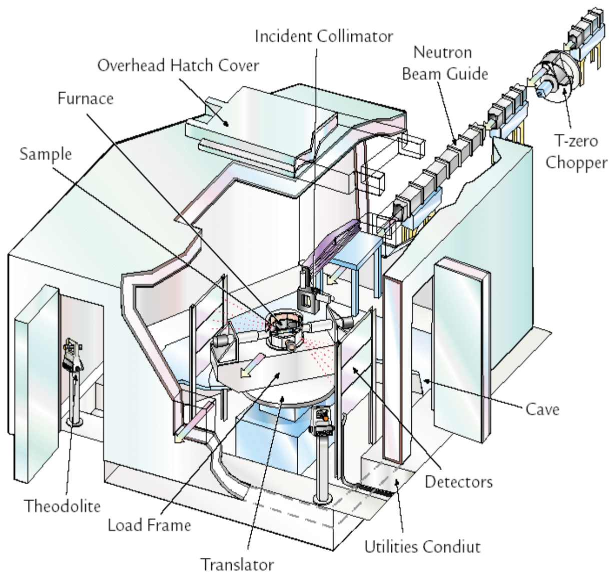

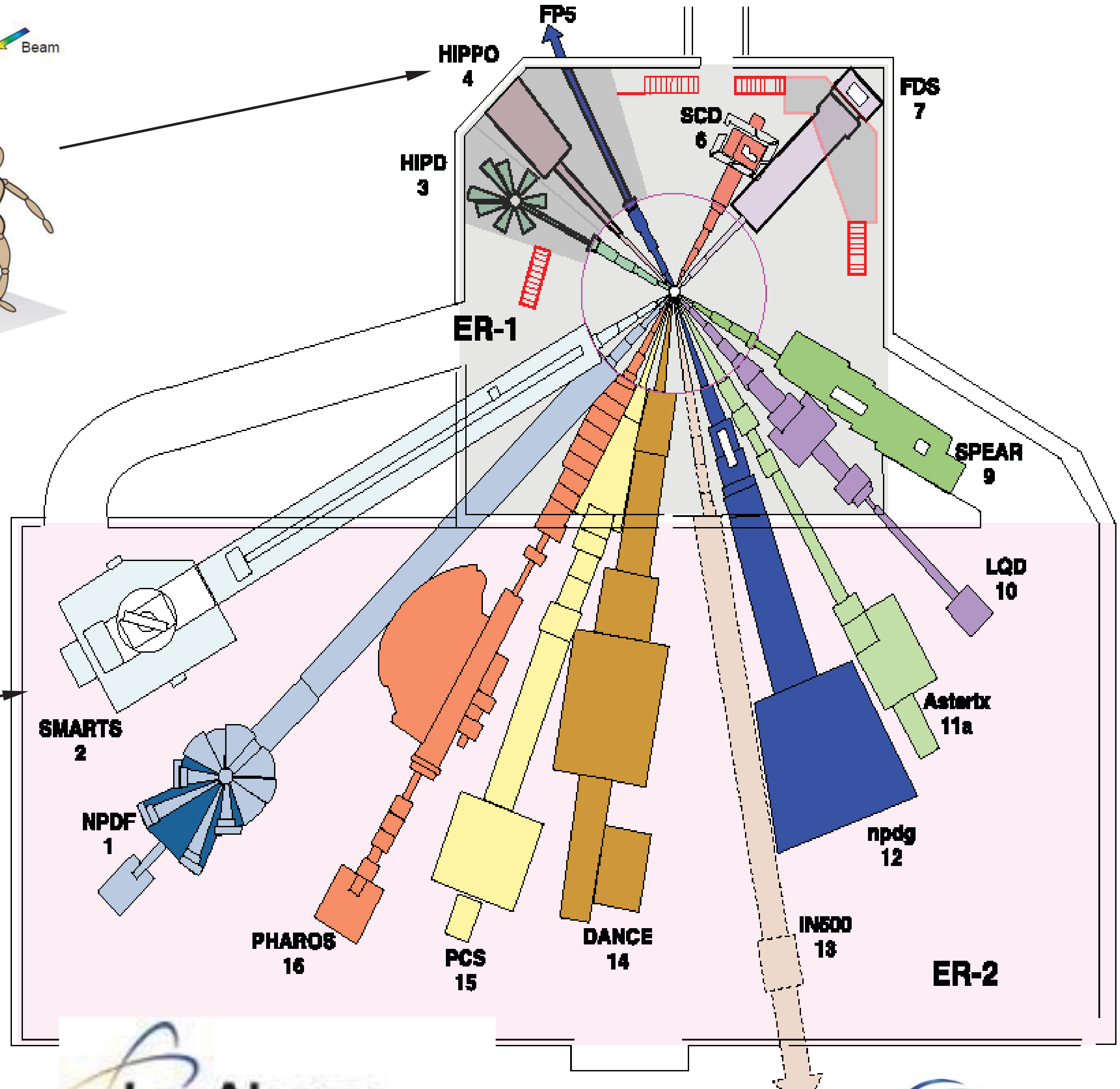

Isothermal Deformation - Loading Actuators

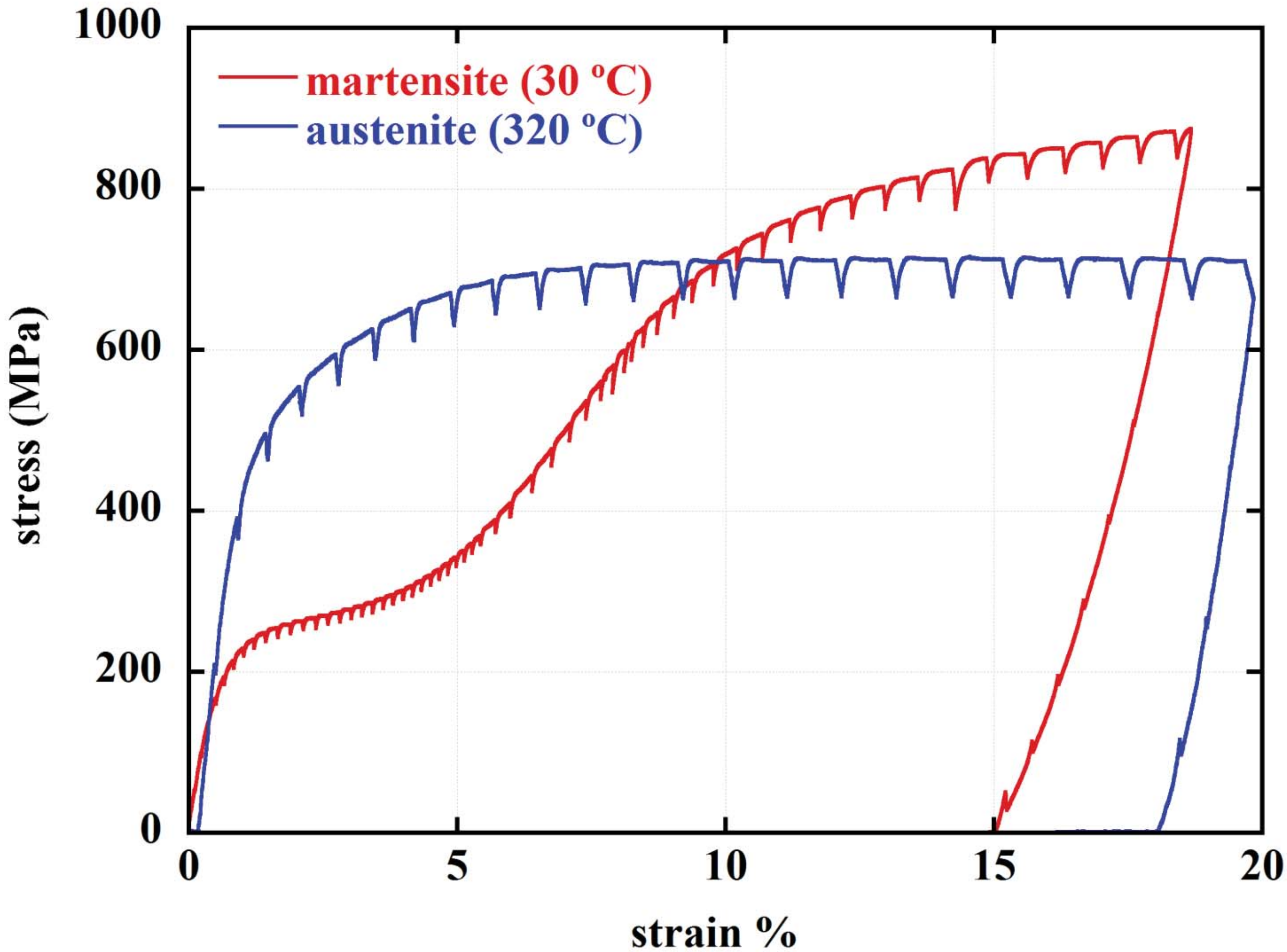

Binary 55NiTi

Isothermal Deformation - Loading Actuators

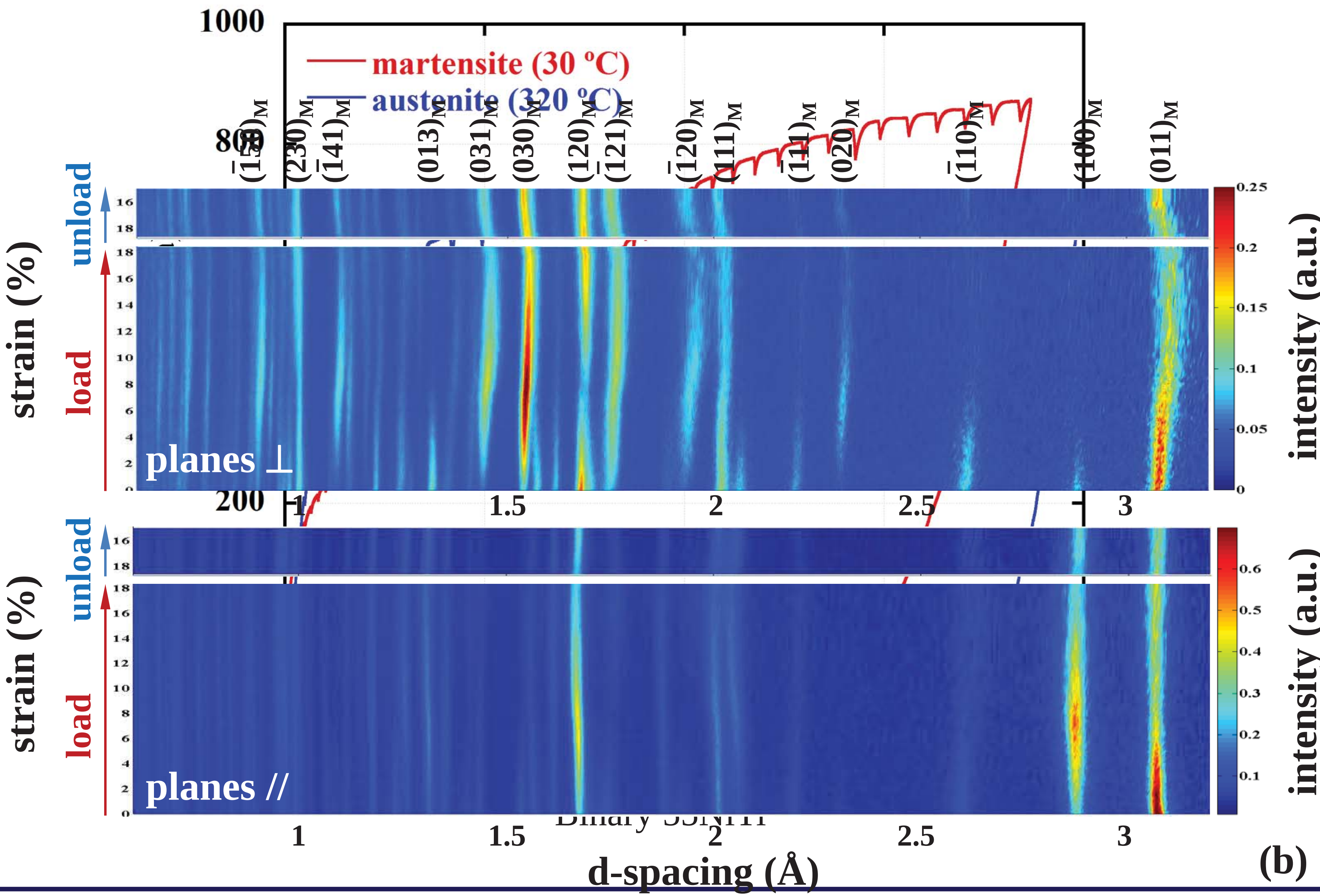

Isothermal Deformation - Loading Actuators

Martensite

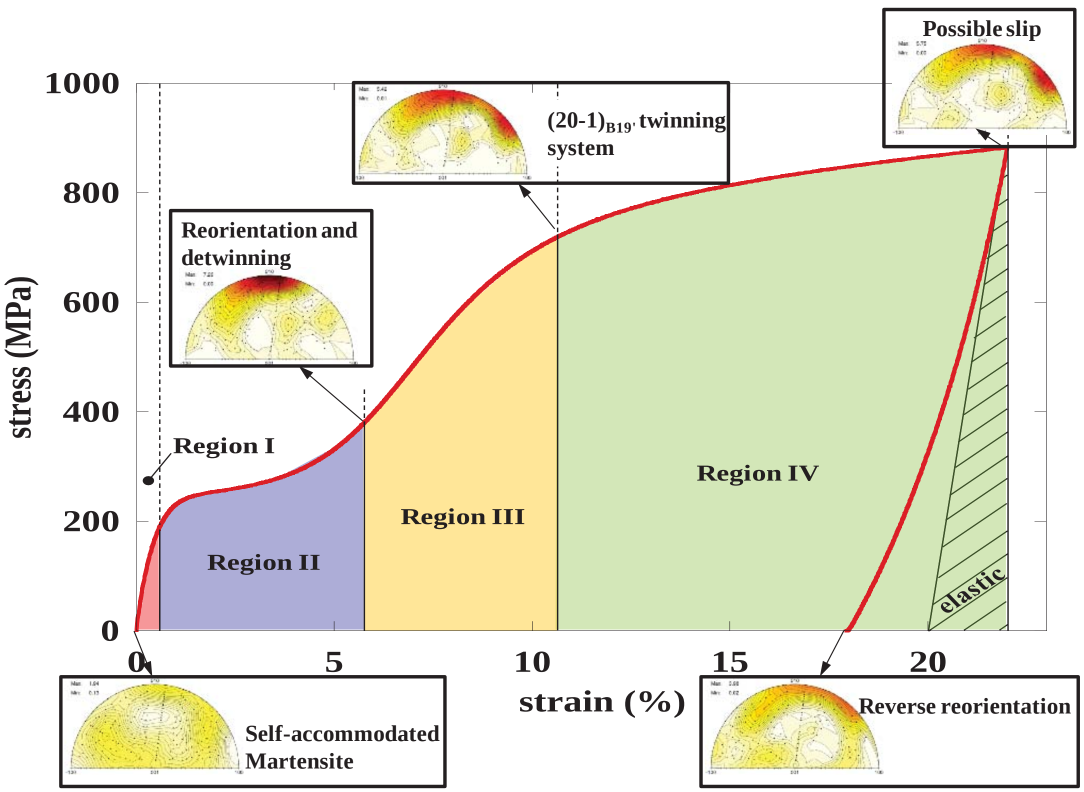

Austenite

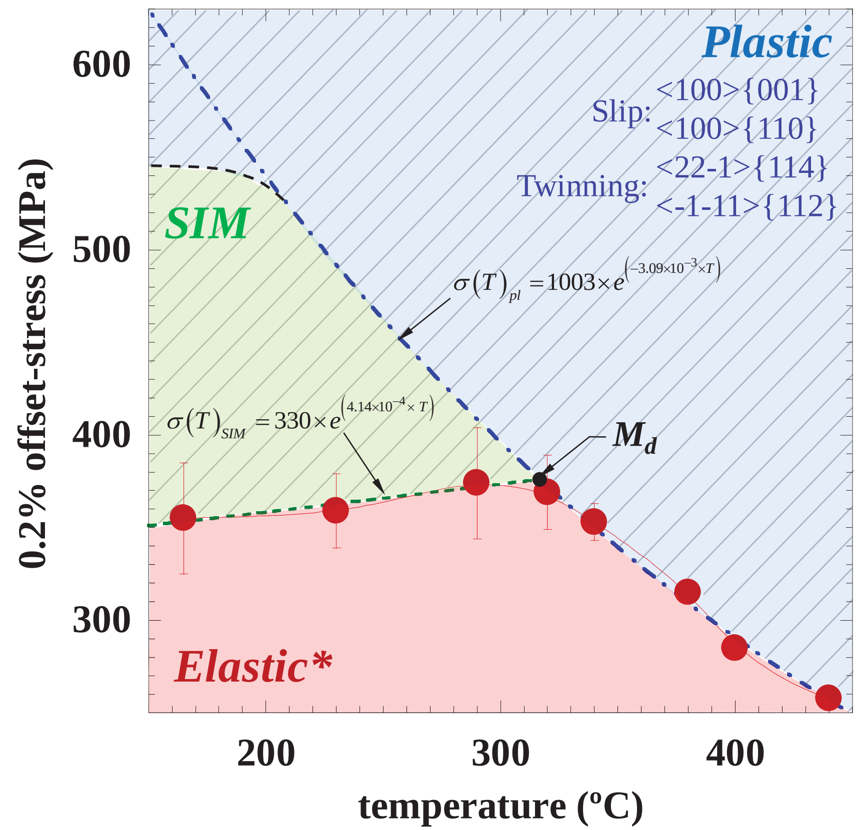

- Deformation mechanisms revealed- complexity and multiplicity of mechanisms can’t be resolved another way
- e.g., reorientation planes/limits, stress- induced-martensite region, martensite desist...

O. Benafan, et al., *Journal of Applied Physics*, 2012, 112, 093510, p. 1–11.

Isothermal Deformation – Where to Load Actuators? Does it Matter?

Loading in martensite

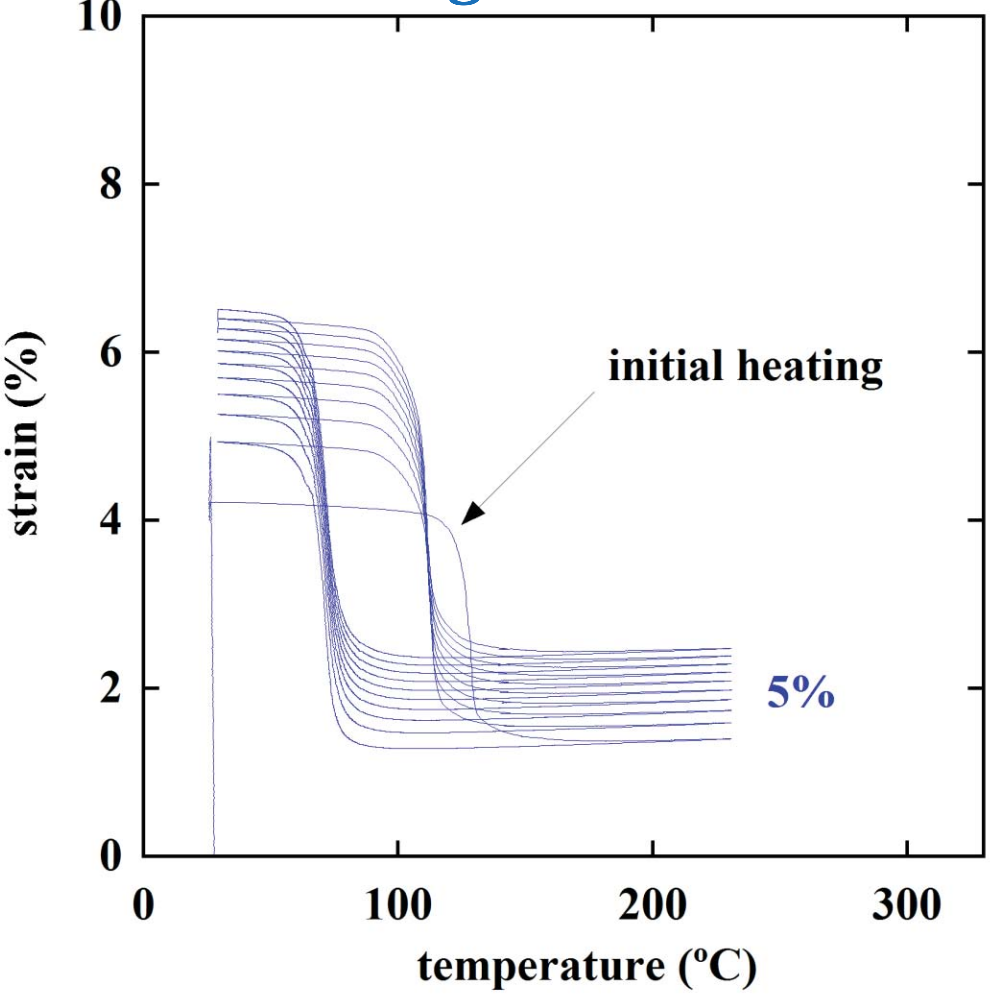

Loading in Austenite

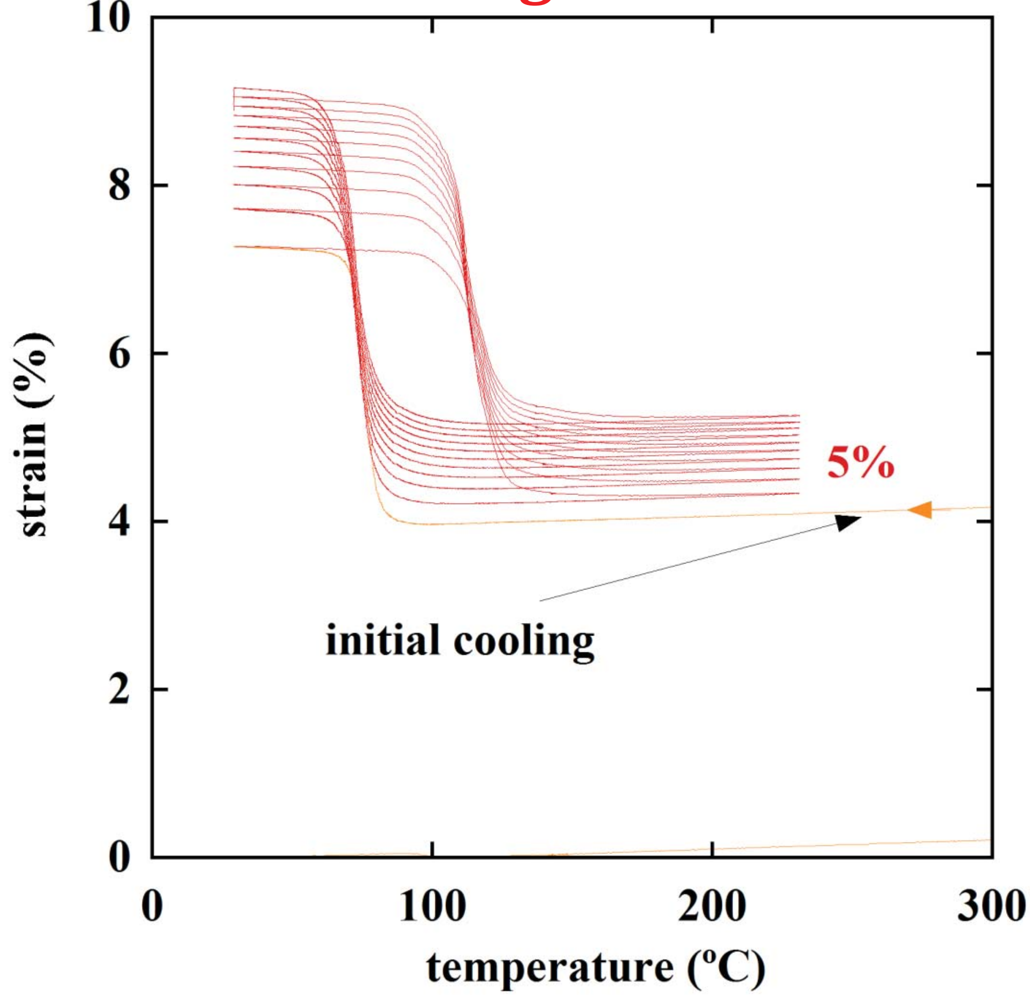

- No major differences in transformation strains
- Large strain evolution (ratcheting) difference

SMA Properties – Can they be Optimized for Actuators?

1. Material and Geometry‡

- Binary 55NiTi → ϕ = 5.08mm (0.2in)
- Stress free transformation temperatures
  - $A_s = 92\ °C$
  - $A_f = 105\ °C$
  - $M_s = 71\ °C$
  - $M_f = 55\ °C$
- Effective coefficient of thermal expansion
  - $\alpha_A^* = 13.0 \times 10^{-6} / °C$
  - $\alpha_M^* = 6.4 \times 10^{-6} / °C$
- Effective elastic moduli
  - $E_A^* = 74\ GPa$
  - $E_M^* = 50\ GPa$
- Effective Poisson's ratios
  - $\nu_A^* = 0.33$
  - $\nu_M^* = 0.387$

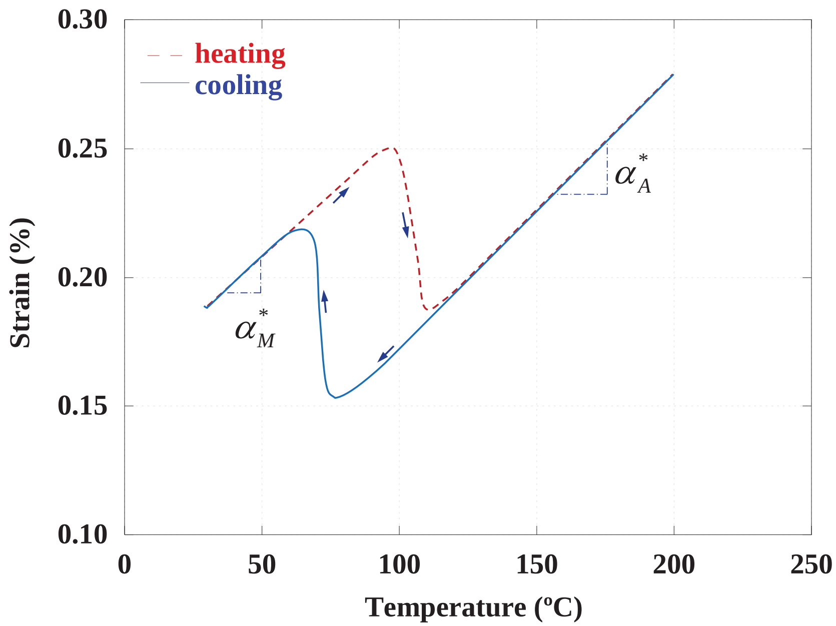

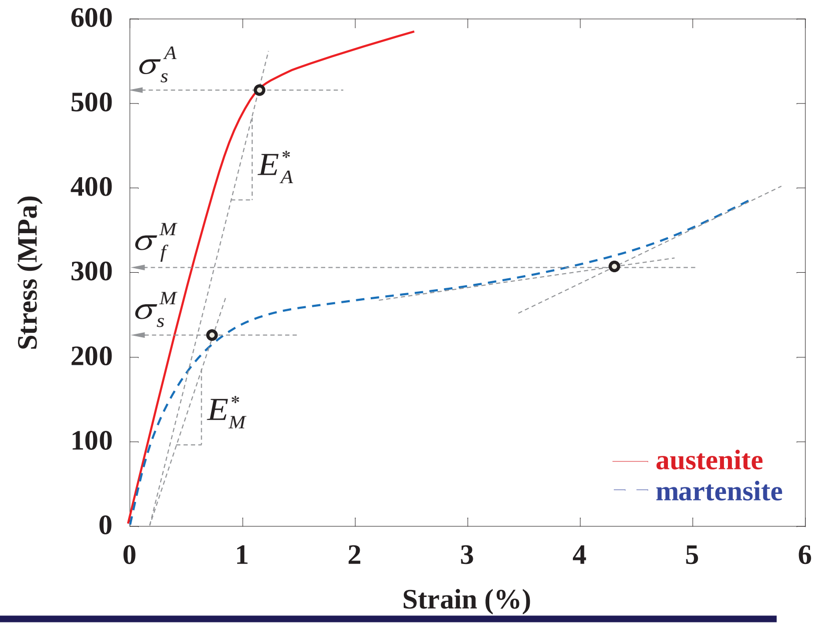

Transformation Temperatures: DSC vs. Strain-Temperature vs. Neutrons

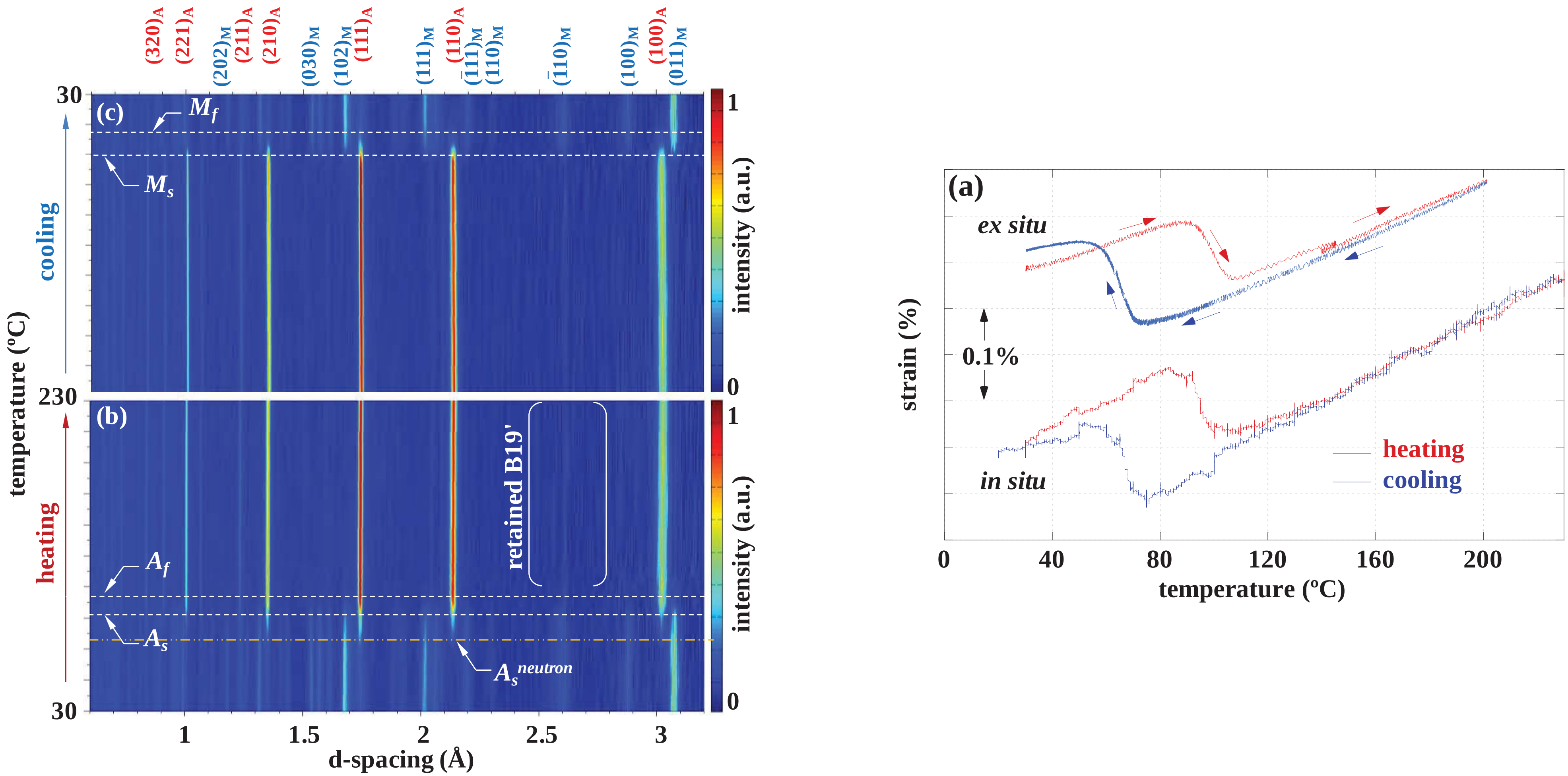

- Transformation temperatures during the reverse transformation measured from strain-temperature and DSC data were found to differ from the actual onset of transformation as revealed from neutron spectra.
- The austenite phase starting to form at ~75 °C,

Dynamic Young's Modulus for $Ni_{49.9}Ti_{50.1}$

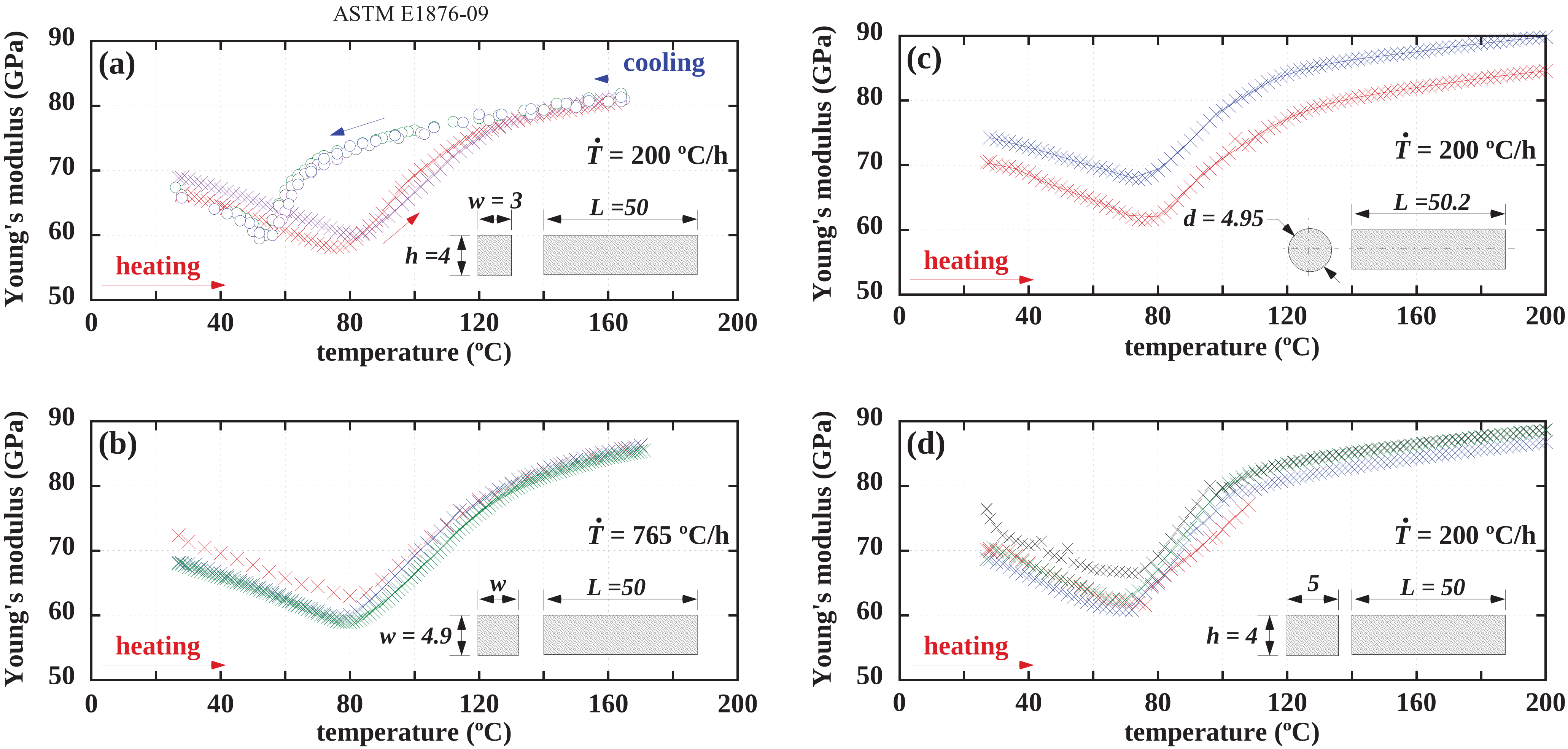

- Dynamic Young's modulus data obtained from the impulse excitation of vibration tests.
- The average dynamic modulus of martensite at room temperature was about 70 GPa, but decreased with increasing temperature with an average minimum value of 60 GPa at ~80 °C.

0.2% Offset "Yield" Stress Behavior of $Ni_{49.9}Ti_{50.1}$

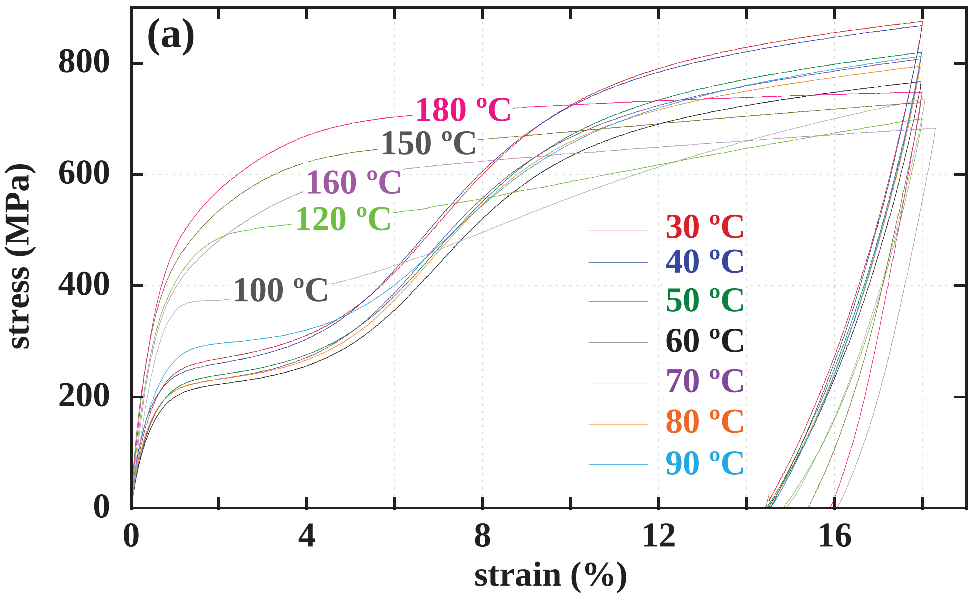

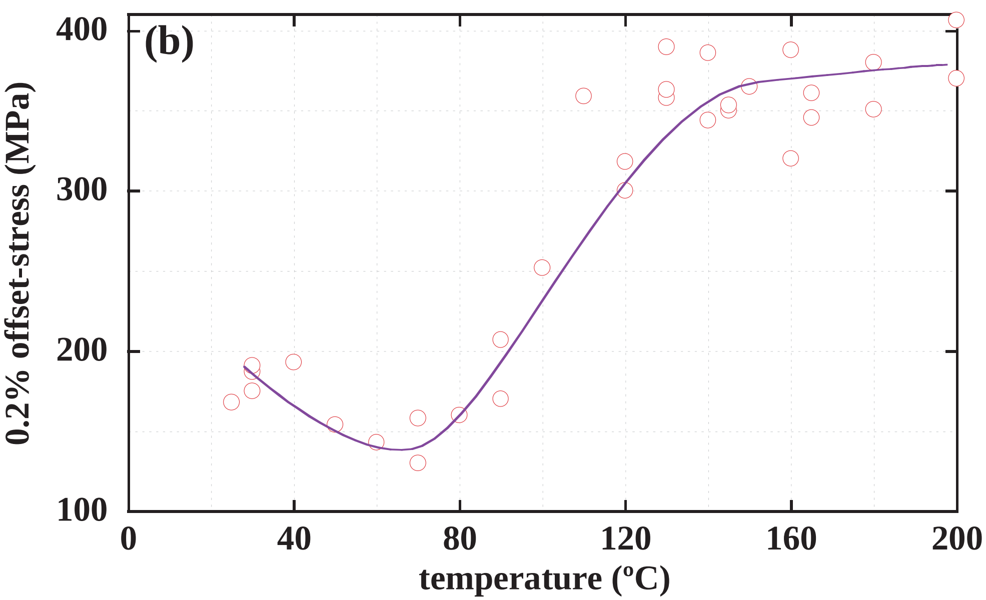

- The onset of inelastic deformation (generally referred to as 'yield') in the martensite phase is dominated by reorientation and detwinning mechanisms.
- Decrease with increasing temperature, reaching an averaged minimum value of 140 MPa between 65 and 80 ºC.
- The onset stress then sharply increased in the two-phase region and reached near saturation (with a still slightly positive slope) at 350 MPa near 130 ºC.
- Inelastic deformation over this temperature range (~90 – 130 ºC), which includes the B19'→ B2 phase transition, is attributed to the nearly concurrent operation of stress-induced martensite and plastic deformation.

Transformation Temperatures: DSC vs. Strain-Temperature vs. Neutrons

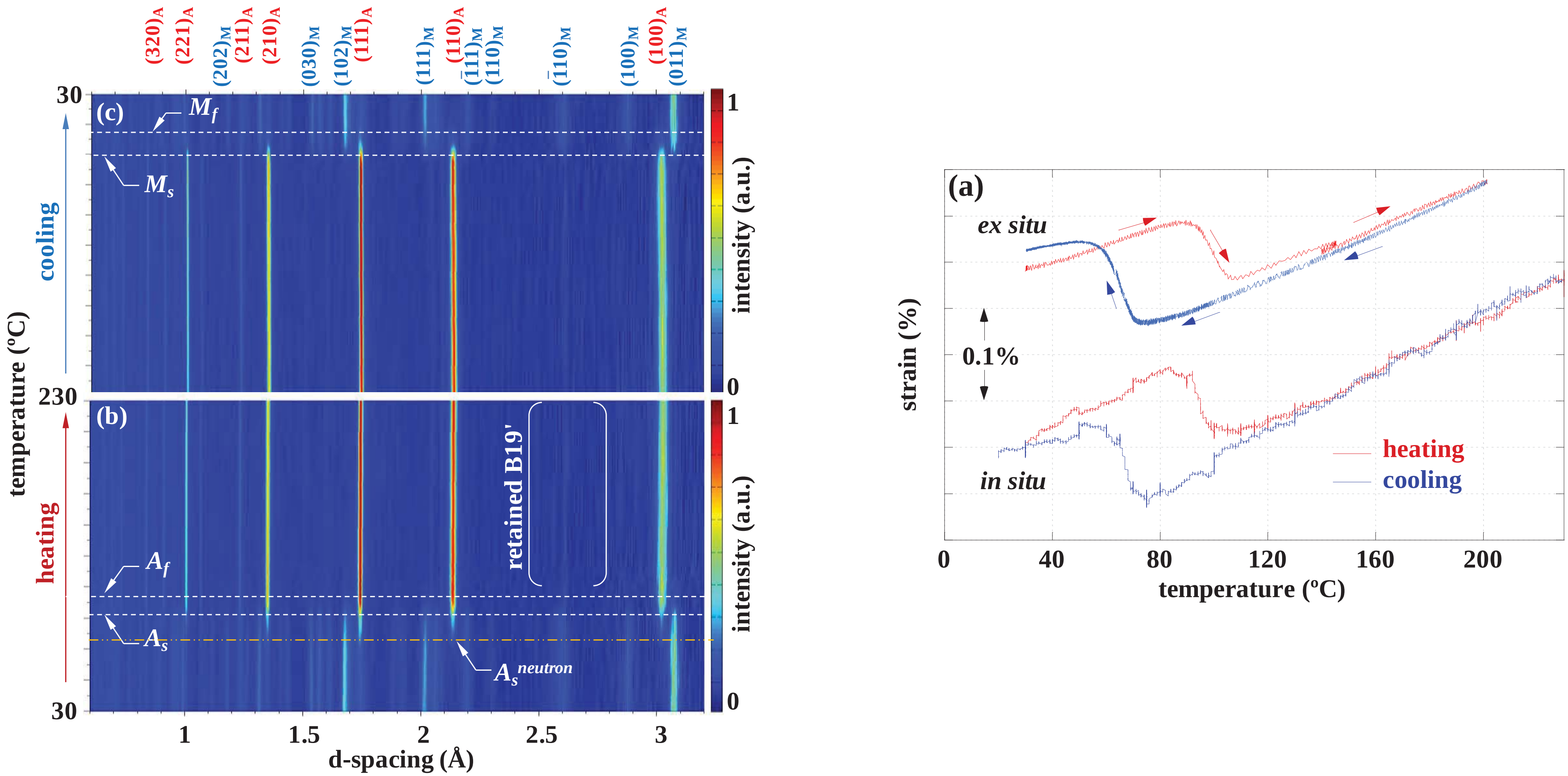

- Transformation temperatures during the reverse transformation measured from strain-temperature and DSC data were found to differ from the actual onset of transformation as revealed from neutron spectra.
- The austenite phase starting to form at ~75 °C,

Thermomechanical Cycling of Actuators

55NiTi

Electron diffraction

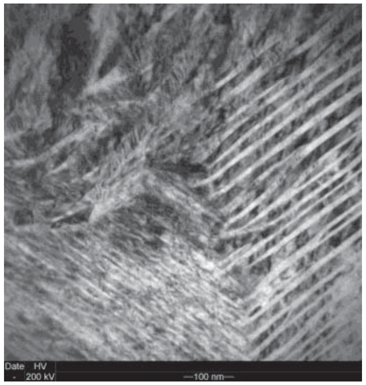

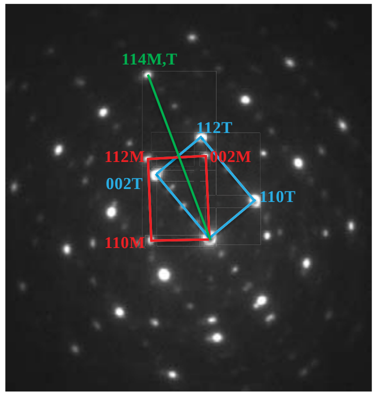

In situ diffraction

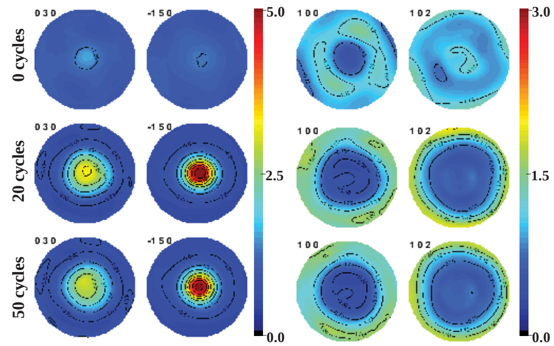

Outcome

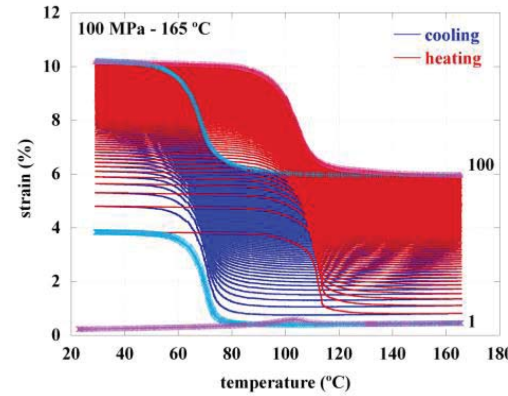

SMA Properties – Can they be Optimized for Actuators?

1. Material and Geometry‡

- Binary 55NiTi → ϕ = 5.08mm (0.2in)
- Stress free transformation temperatures
  - $A_s = 92\ °C$
  - $A_f = 105\ °C$
  - $M_s = 71\ °C$
  - $M_f = 55\ °C$
- Effective coefficient of thermal expansion
  - $\alpha_A^* = 13.0 \times 10^{-6}\ / °C$
  - $\alpha_M^* = 6.4 \times 10^{-6}\ / °C$
- Effective elastic moduli
  - $E_A^* = 74\ GPa$
  - $E_M^* = 50\ GPa$
- Effective Poisson's ratios
  - $\nu_A^* = 0.33$
  - $\nu_M^* = 0.387$

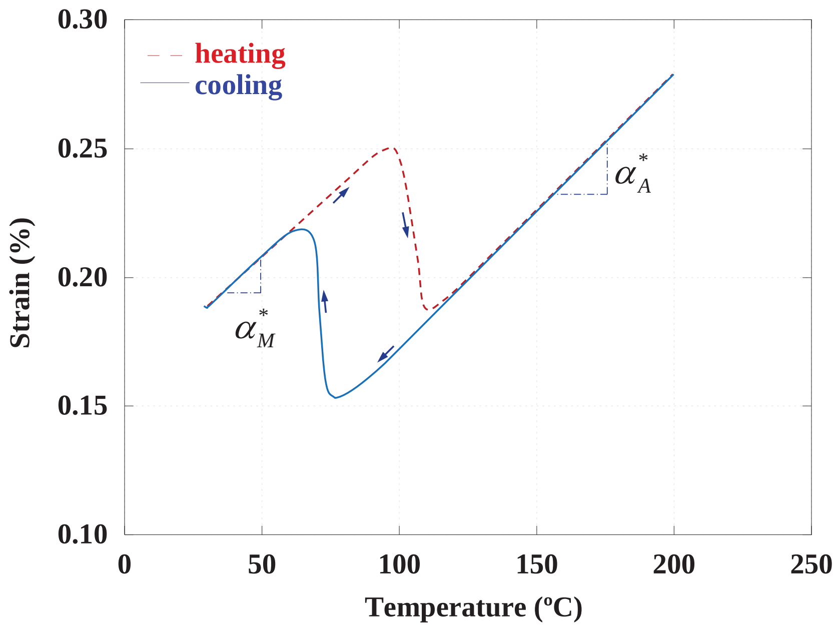

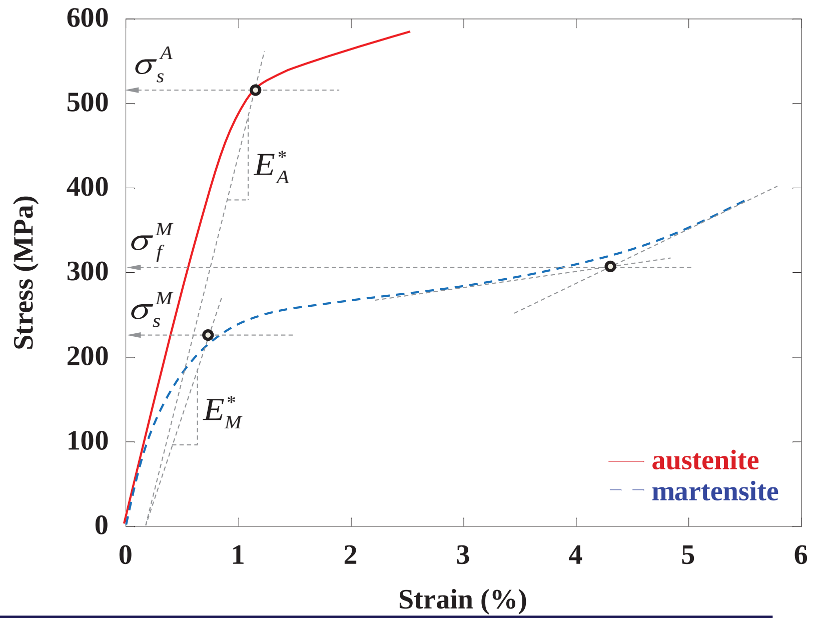

Coefficient of Thermal Expansion: Large Anisotropy

- Atomic scale measurements of thermal strains

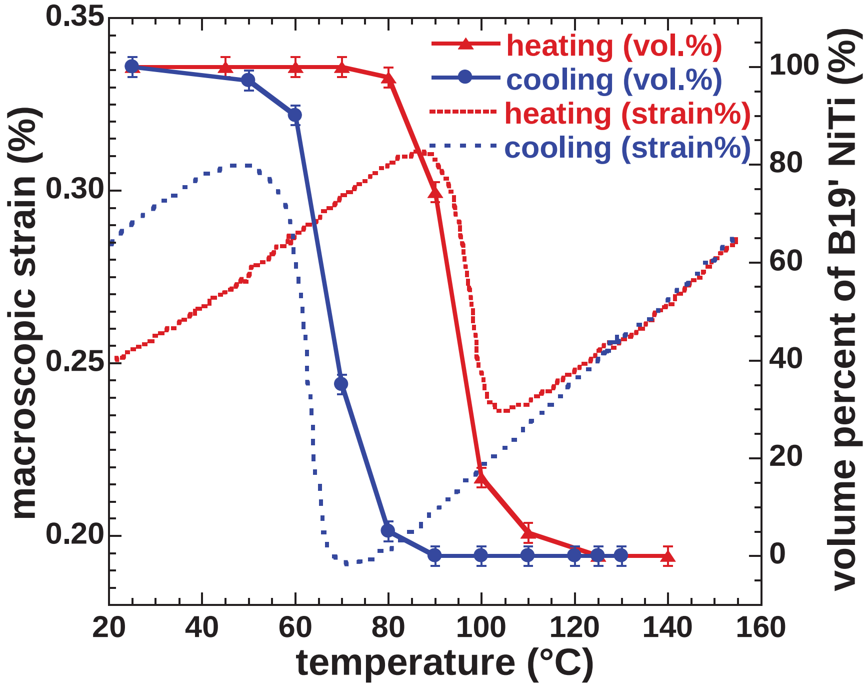

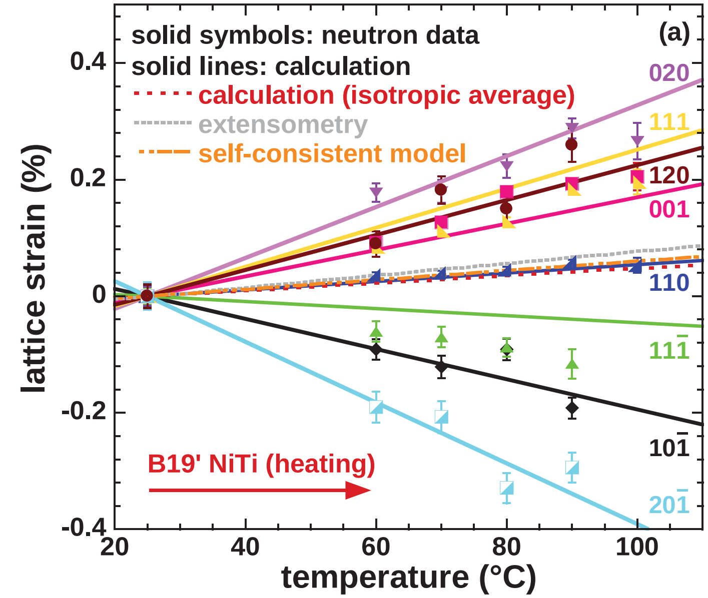

			Heating (10^{-6}/°C)	Cooling (10^{-6}/°C)
B19' NiTi	Thermal expansion tensor components	α_{11}	-47.2	-30.8
		α_{22}	43.8	32.1
		α_{33}	22.7	27.3
		α_{31}	29.0	32.4
	CTE*		6.4	9.5
	CTE†		8.1	10.9
	CTE (extensometry)		10.3	9.0
B2 NiTi	CTE*		13.0	13.1
	CTE (extensometry)		12.4	12.3

*isotropic average †self-consistent model

- **Outcome**
  - First report on NiTi CTE tensor (monoclinic martensite) including negative expansion in certain crystal orientations
  - Parametric input for most SMA models

[1] S. Qiu et al., Appl. Phys. Lett. 95, 141906 (2009)

Coefficient of Thermal Expansion: Large Anisotropy

- Similar observation in HTSMAs (e.g., NiTiPt – B19)

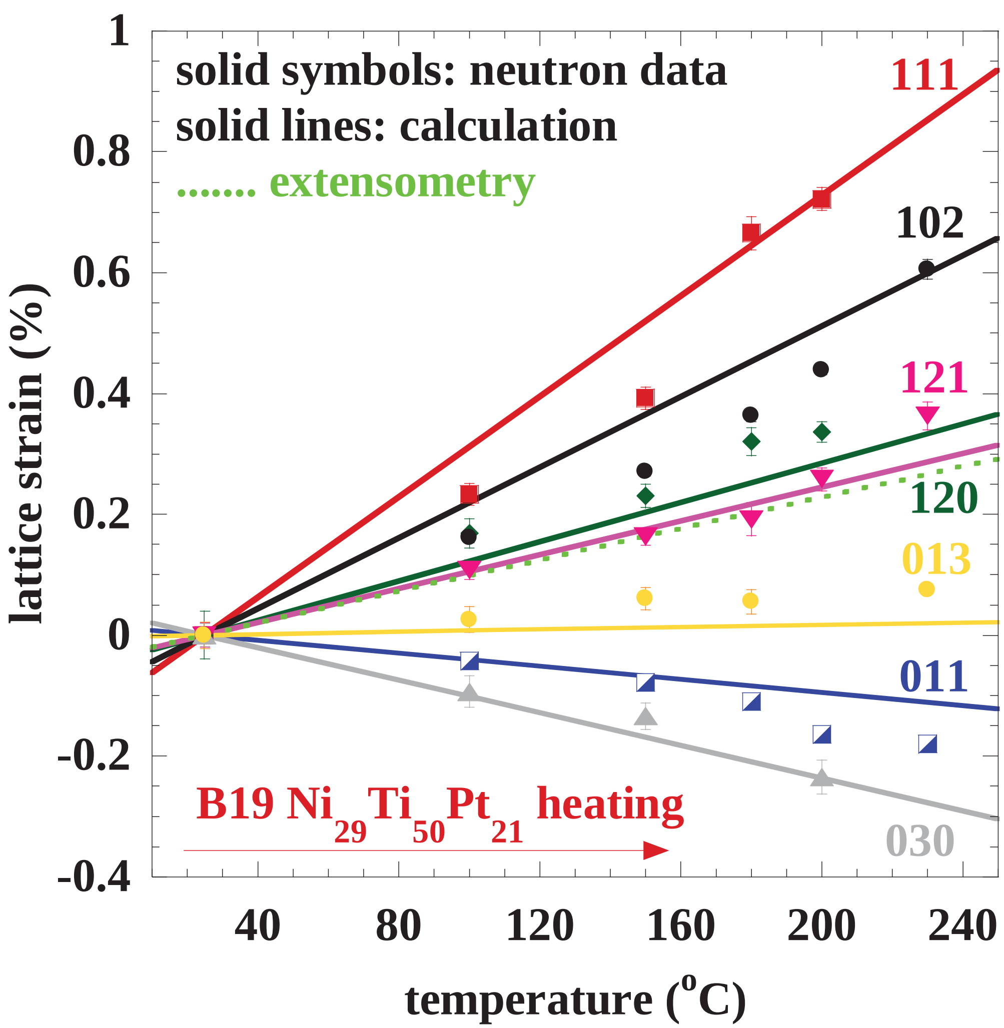

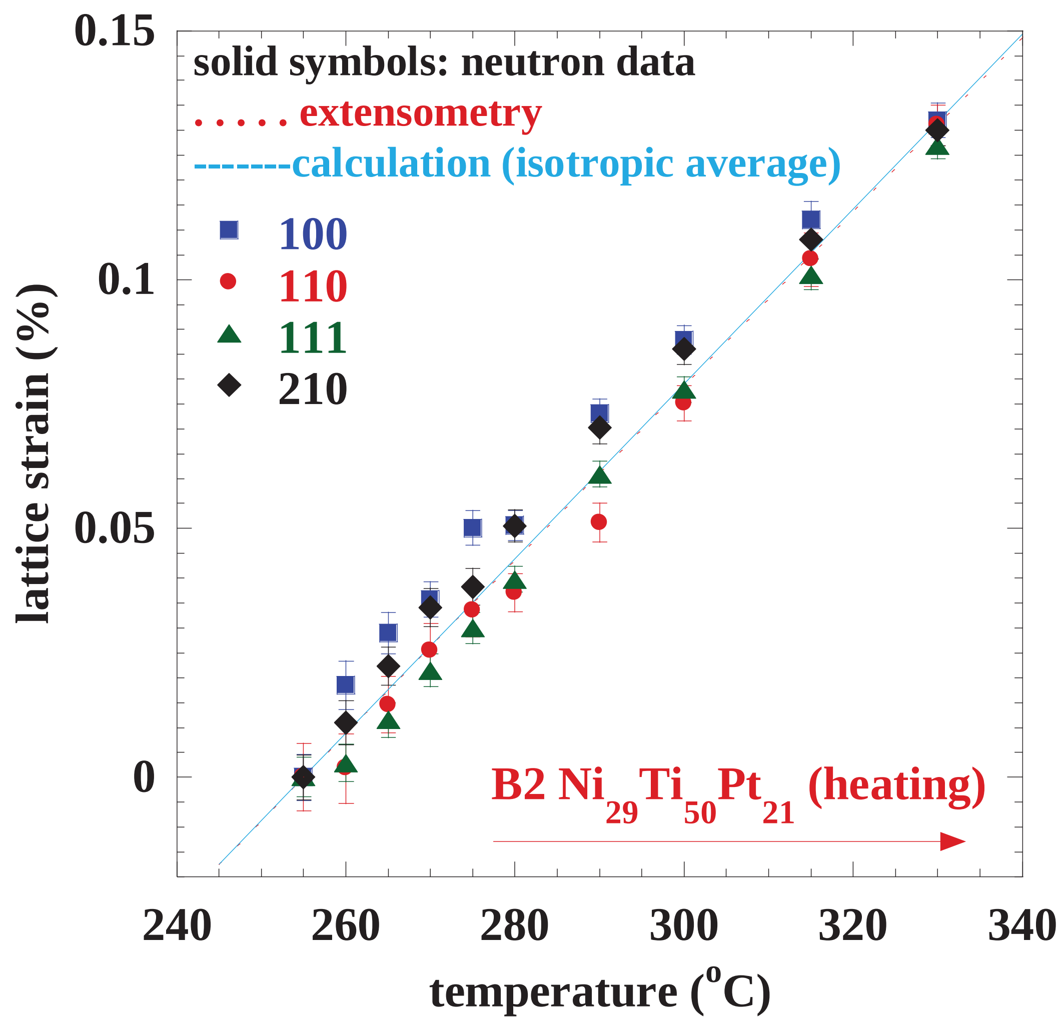

O. Benafan et al., unpublished work

SMA Properties – Can they be Optimized for Actuators?

1. Material and Geometry‡

- Binary 55NiTi → ϕ = 5.08mm (0.2in)
- Stress free transformation temperatures
  - $A_s = 92\ °C$
  - $A_f = 105\ °C$
  - $M_s = 71\ °C$
  - $M_f = 55\ °C$
- Effective coefficient of thermal expansion
  - $\alpha_A^* = 13.0 \times 10^{-6} / °C$
  - $\alpha_M^* = 6.4 \times 10^{-6} / °C$
- Effective elastic moduli
  - $E_A^* = 74\ GPa$
  - $E_M^* = 50\ GPa$
- Effective Poisson's ratios
  - $\nu_A^* = 0.33$
  - $\nu_M^* = 0.387$

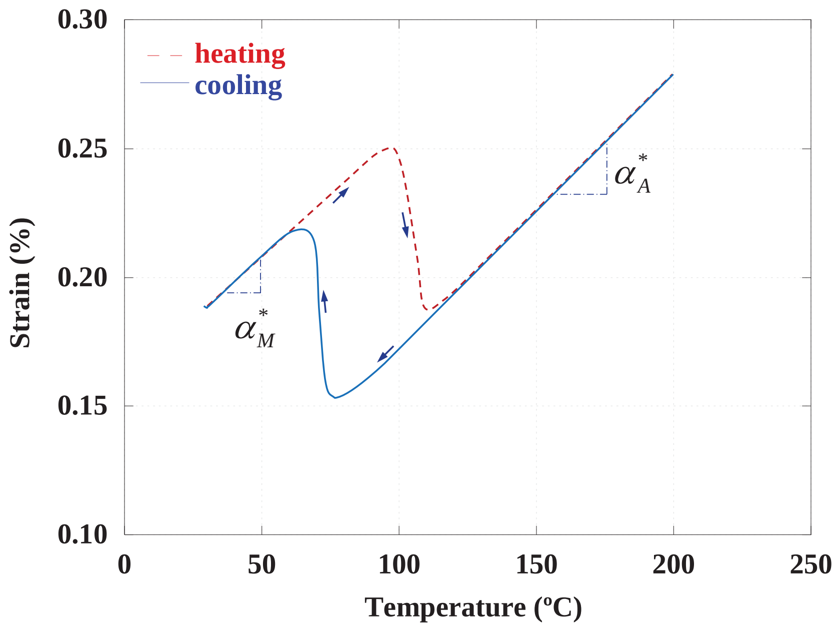

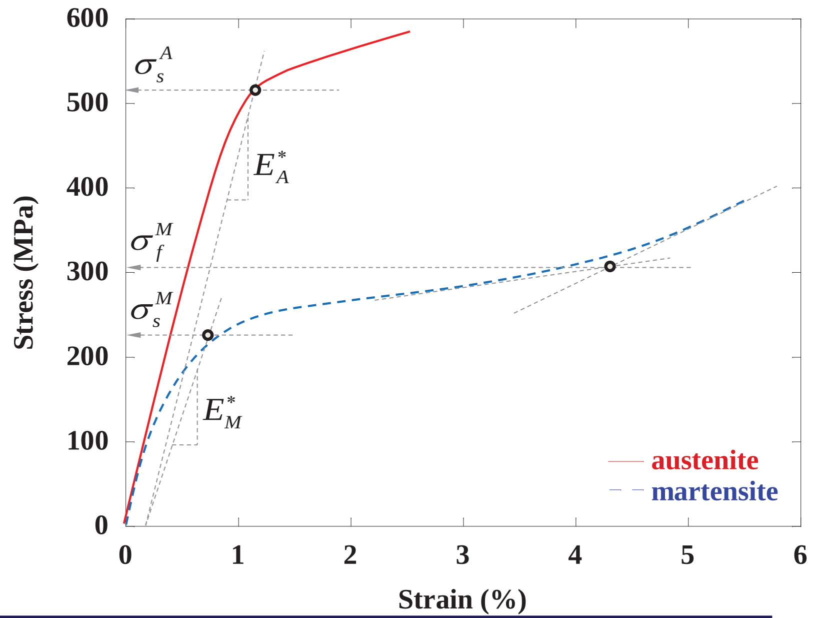

Elastic Moduli: Hard and Soft Orientations

- Strain anisotropy and texture measurements

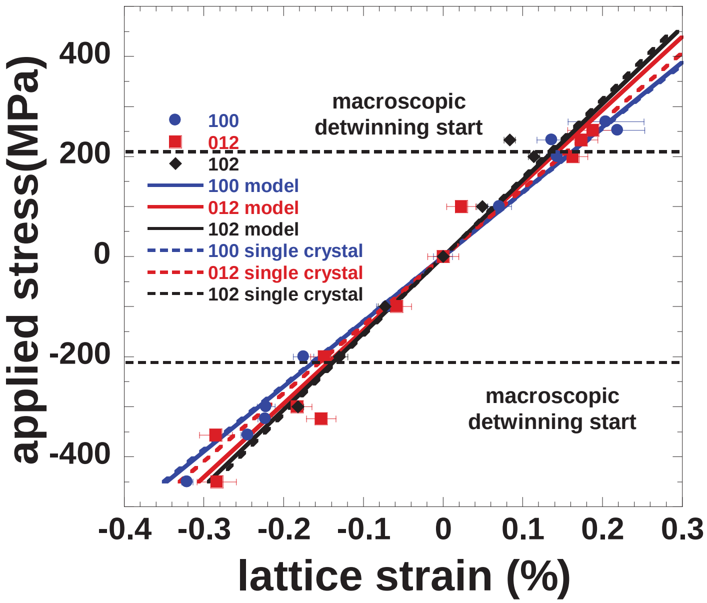

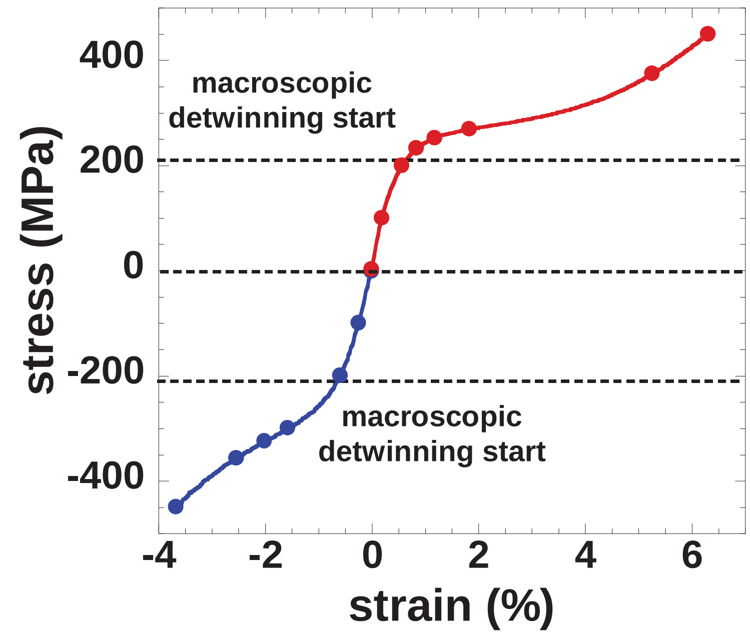

hkl	Single crystal $E_{hkl}^{crystal}$	Model E_{hkl}^{model}	Neutron diffraction $E_{hkl}^{neutron}$	# of points	R
100	128.2	129.8	132.2	6	0.997
012	136.0	146.7	145.4	6	0.978
102	157.3	152.8	167.1	6	0.999
-120	33.8	106.0	101.4	6	0.997
121	84.2	116.3	104.6	6	0.996
-112	177.6	147.6	165.1	6	0.999
-122	120.2	143.7	110.5	5	0.991
-111	85.9	130.2	104.7	5	0.999
011	175.9	155.7	117.1	6	0.995
-121	53.4	122.0	93.3	5	1.000
-110	41.0	105.1	78.2	6	0.997

- **Outcome**
  - First validation of *ab initio* calculation
  - Entire compliance matrix, not just a Young's modulus
  - Revealed mechanisms responsible for deflated modulus values obtained from conventional macroscopic tests

[1] S. Qiu et al., Acta Mat., 2010

Elastic Moduli: Hard and Soft Orientations

NiTiPt

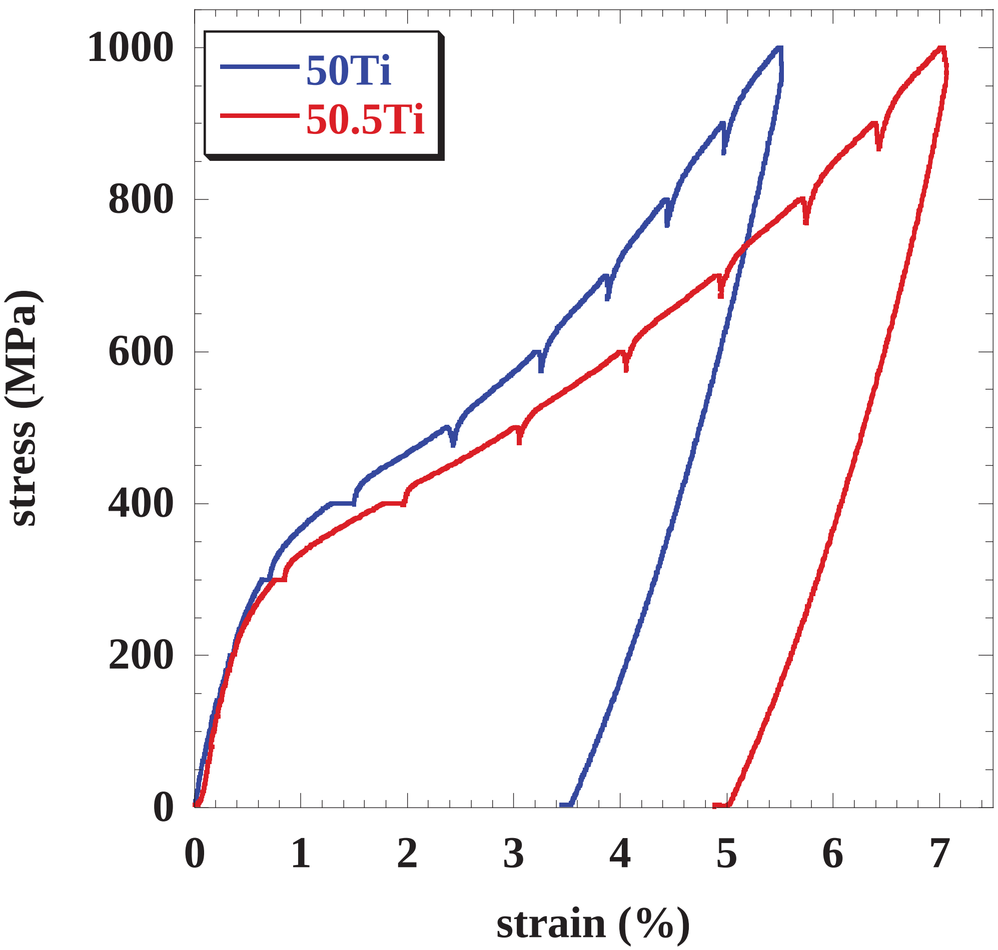

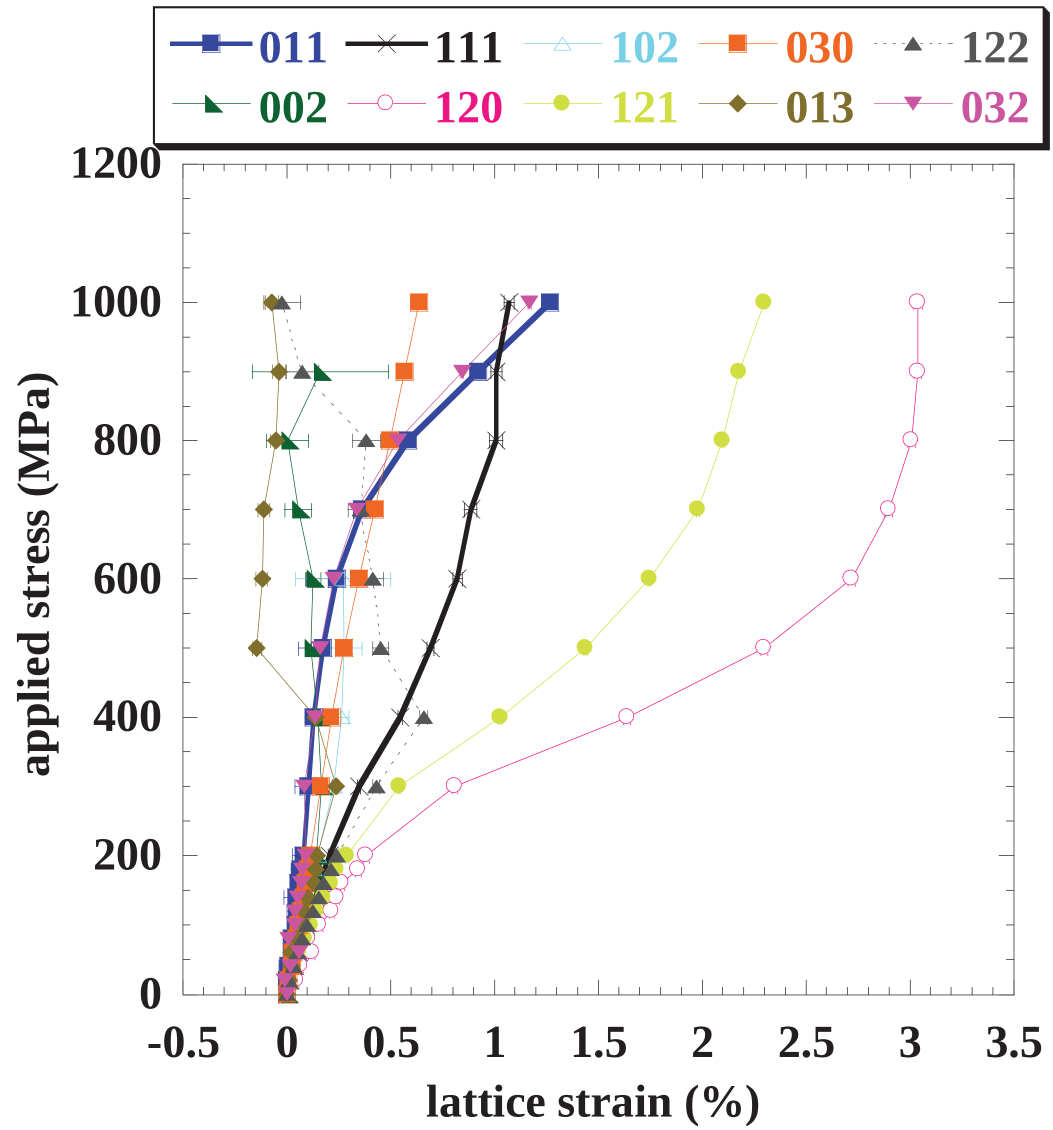

O. Benafan et al., unpublished work

Elastic Moduli: Hard and Soft Orientations

NiTiPt

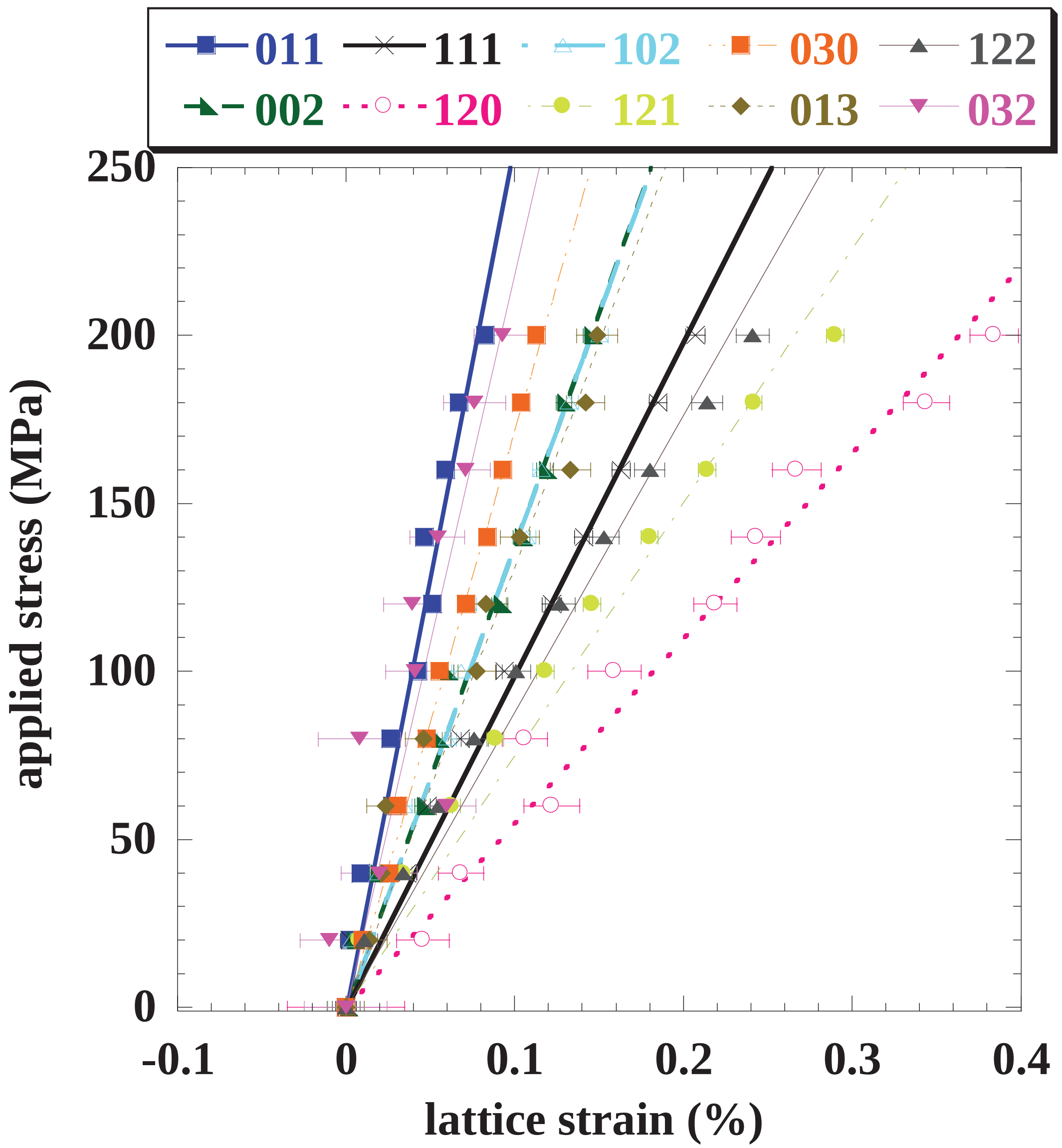

E_{011}=257.8 GPa	R=0.985
E_{002}=138.7 GPa	R=0.994
E_{111}=99.2 GPa	R=0.997
E_{120}=55.1 GPa	R= 0.988
E_{102}=138.3 GPa	R=0.993
E_{121}=75.3 GPa	R=0.995
E_{030}=173.0 GPa	R=0.998
E_{013}=132.3 GPa	R=0.988
E_{122}=88.3 GPa	R=0.996
E_{032}=218.6 GPa	R=0.886

Optimization of Two-Way Shape Memory Effect

- Uniaxial deformation at room temperature followed by free recovery

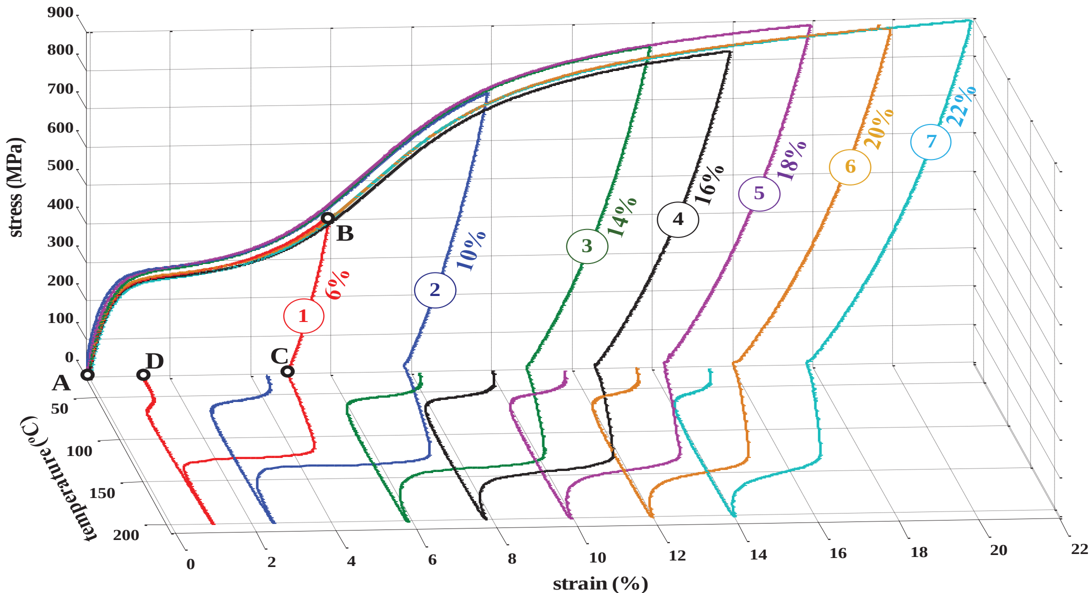

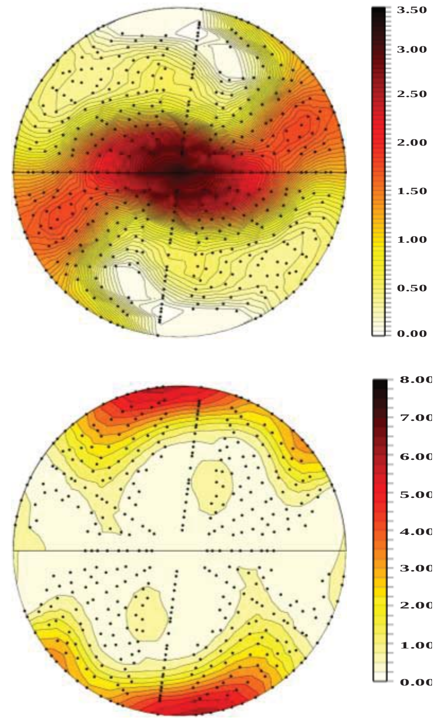

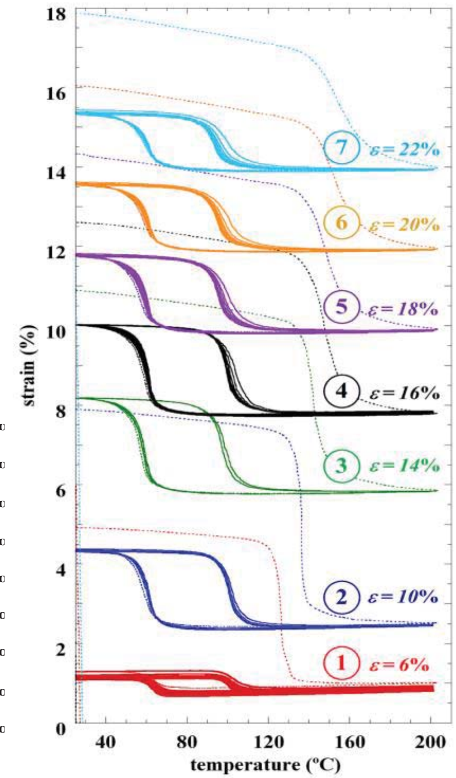

- **Outcome**
  - Established a quick and efficient method for creating a strong and stable TWSME
  - Texture maps were used to determine deformation modes – correlated with TWSME stability and magnitude (not possible another way)

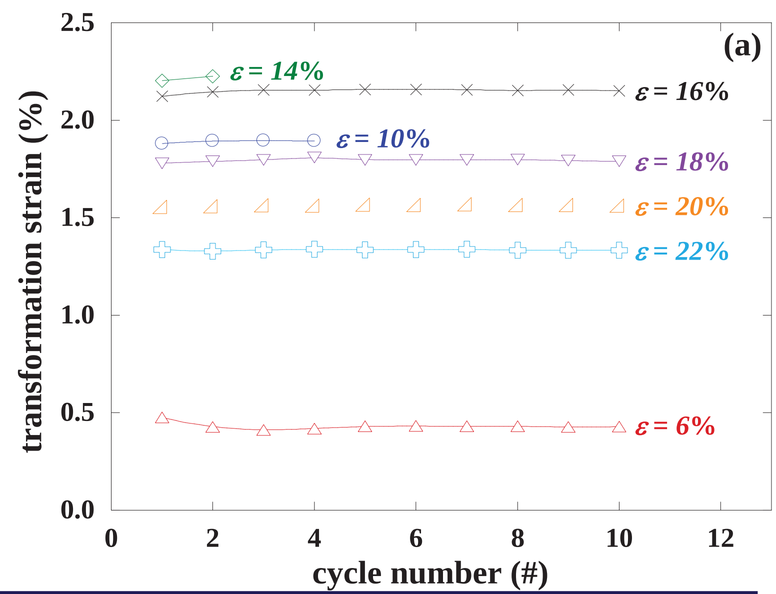

Shape Setting of SMA Actuators

- In situ neutron diffraction during shape setting of bulk polycrystalline NiTi

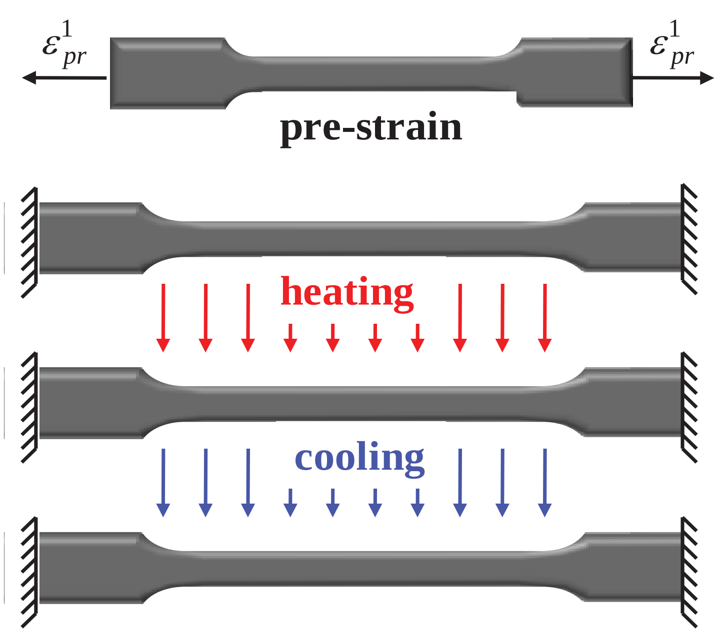

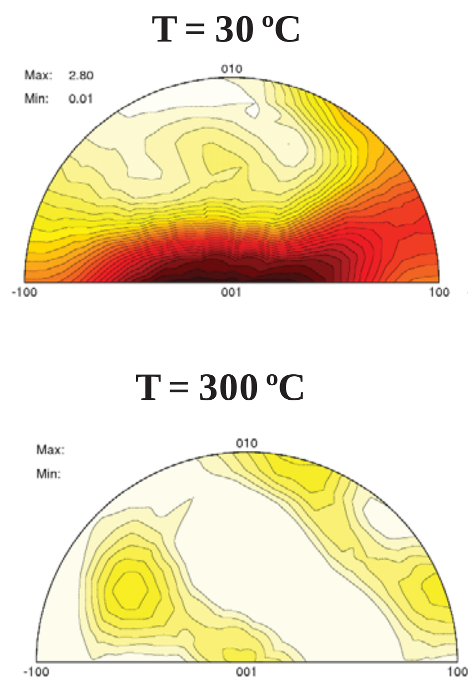

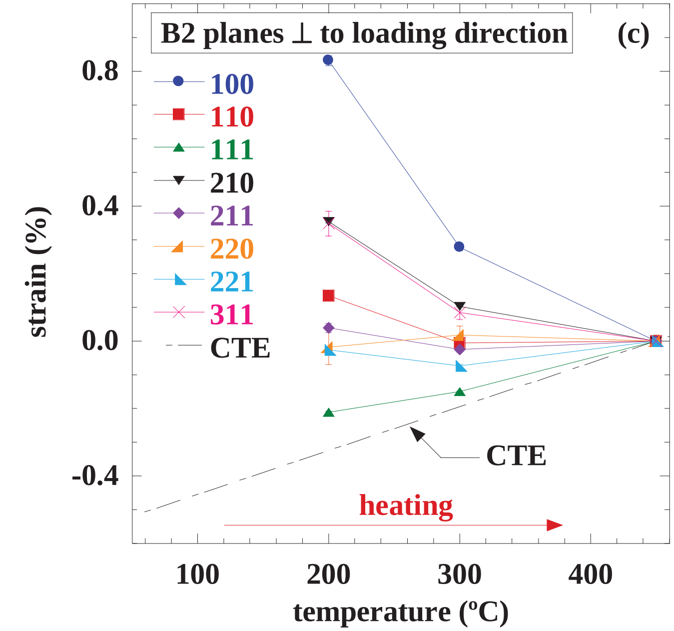

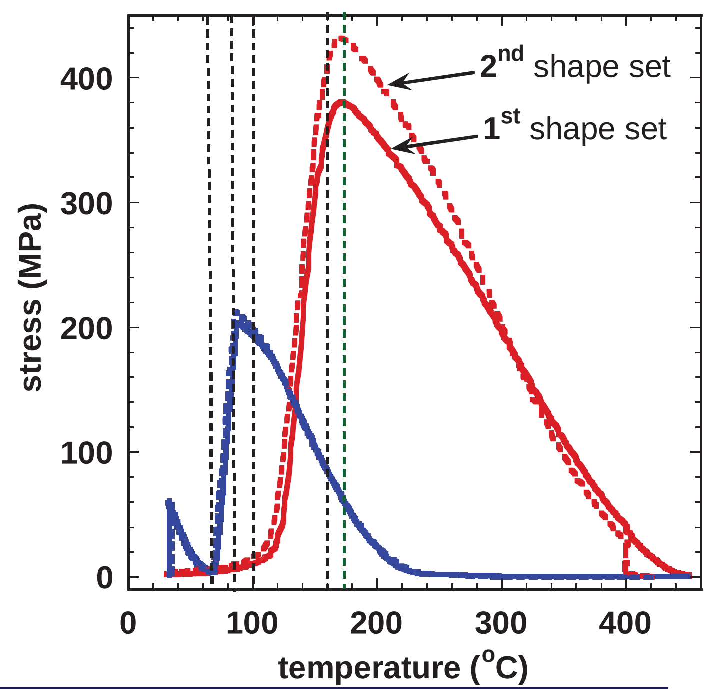

- **Outcome**
  - Guidelines for shape setting any actuator: stress and temperature limits for shape setting
  - Neutrons revealed mechanisms responsible for the stress generation and relaxation during shape setting.

[1] O. Benafan et al. (2012)

Torsional Characteristics of 55NiTi

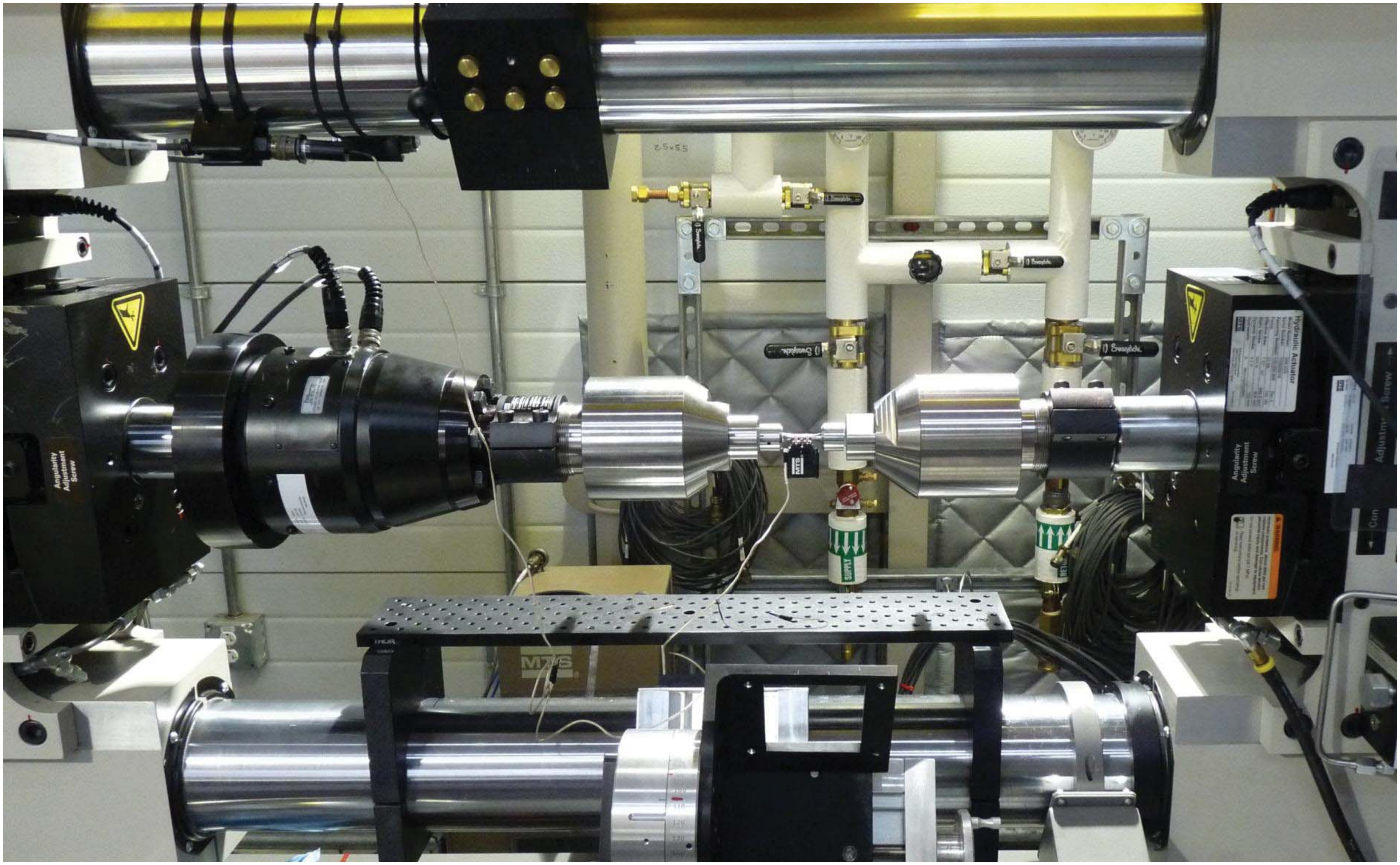

Torsional Characteristics of 55NiTi

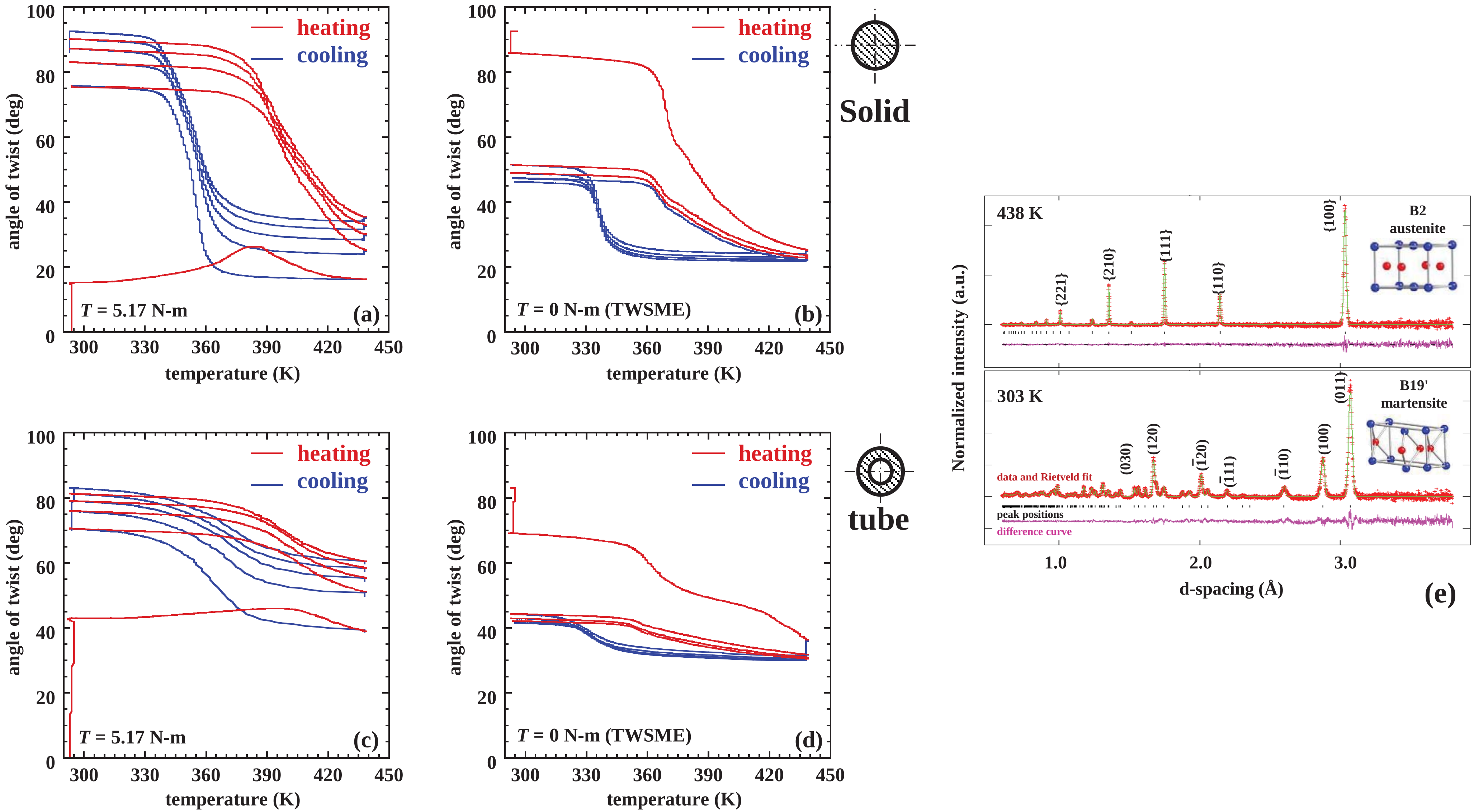

Extension of Neutrons to Novel High Temperature SMAs

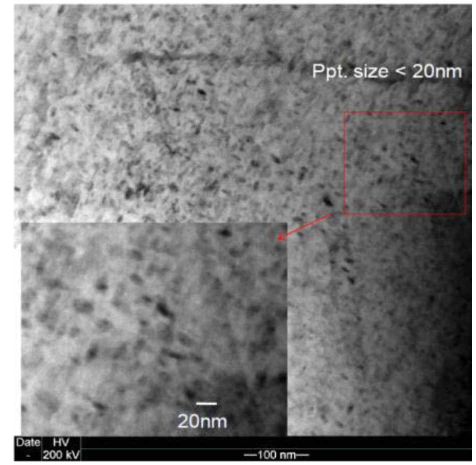

- Microstructural evolution during isothermal and isobaric deformation of NiTiHf

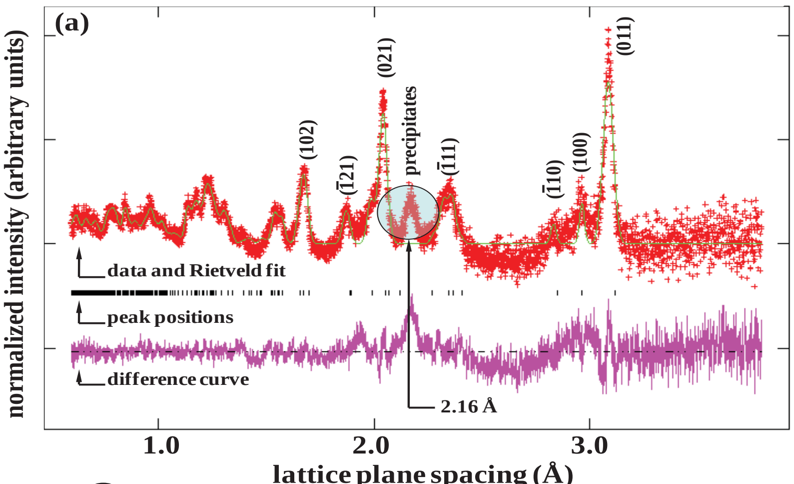

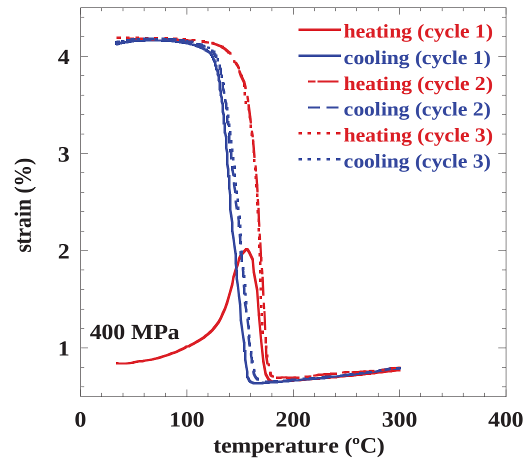

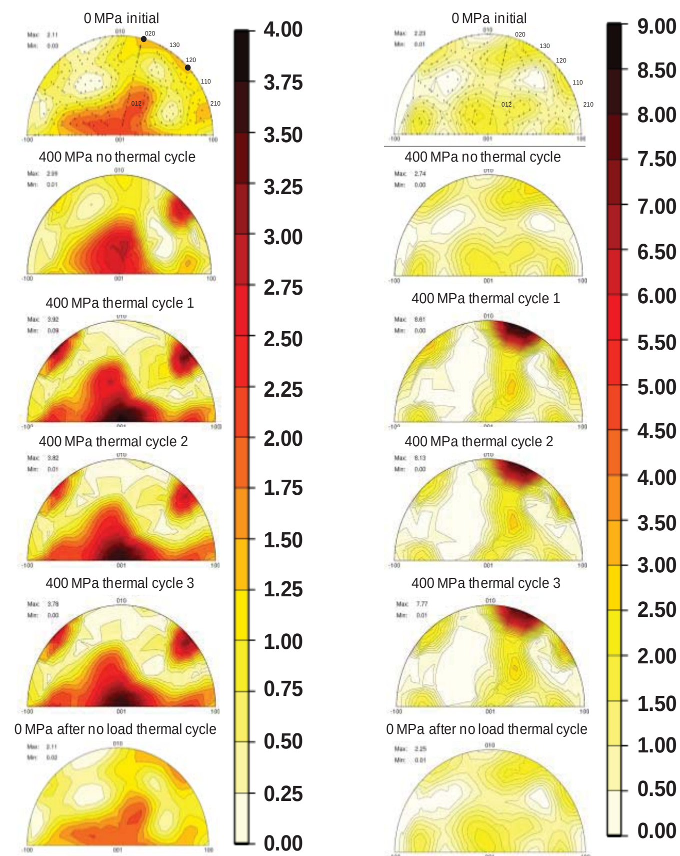

- **Outcome**
  - High work output and dimensional stability
  - Texture measurements were correlated to the lack of evolution in this alloy
  - Confirmed relationship of microstructure and load-biased tests: From Neutron spectra
  - Neutrons showed why training of Hf alloy is not necessary

[1] O. Benafan et al. Metall. Trans. A, 43, 4539 (2012)

Extension of Neutrons to Novel High Temperature SMAs

- The role of retained martensite during thermal-mechanical cycling in NiTiPd high temperature shape memory alloy was revealed

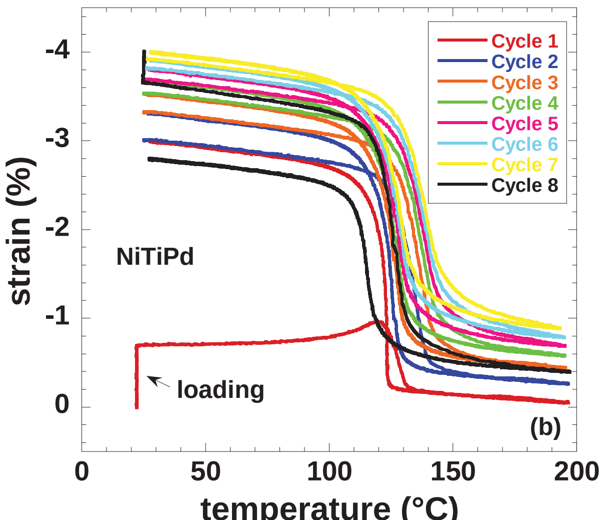

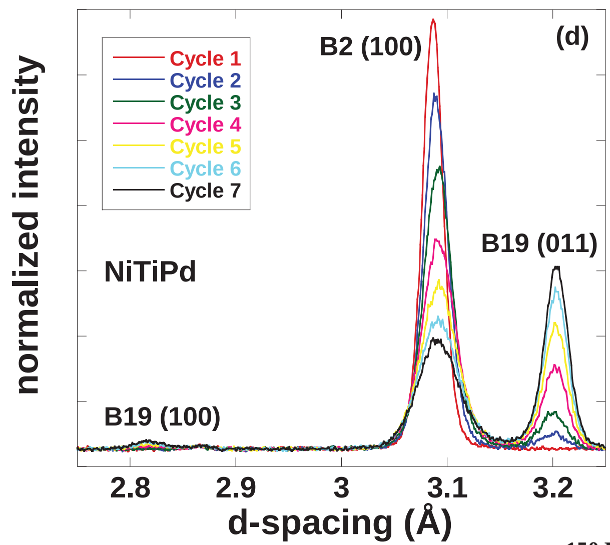

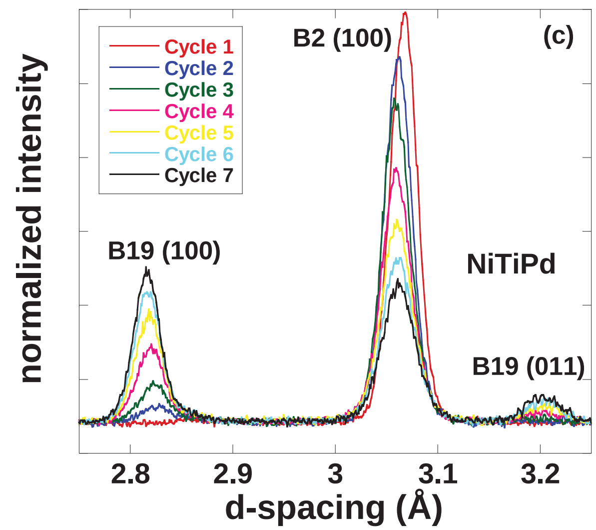

- **Outcome**
  - Direct correlations were made between macroscopic changes in actuator performance parameters, and atomic-scale evolution from neutron spectra
  - The rate of evolution of texture and volume fraction of the retained martensite plays a key role in the stability of the actuator

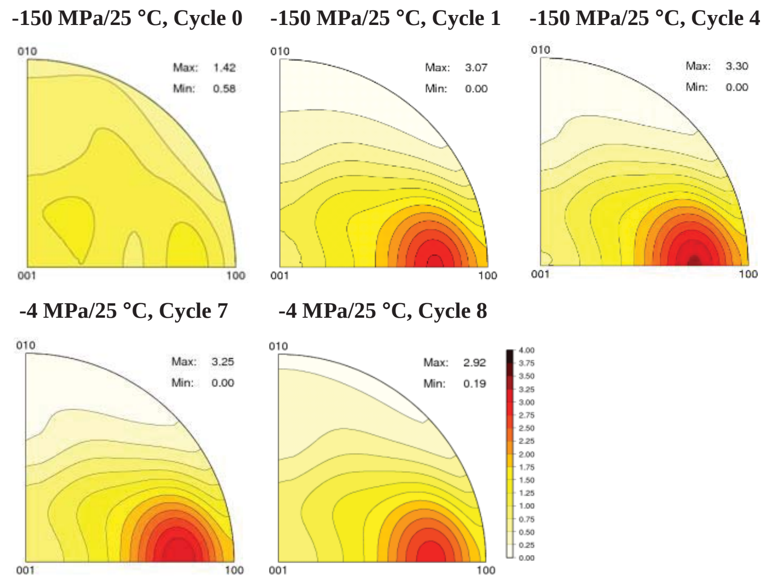

S. Qiu et al.,

Neutrons can be used to study most actuator forms

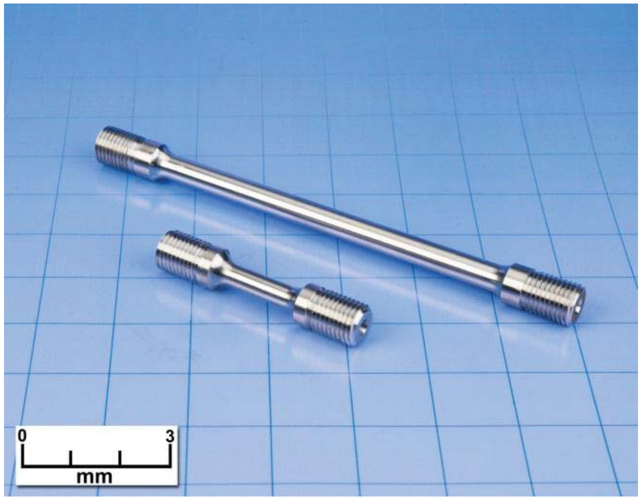

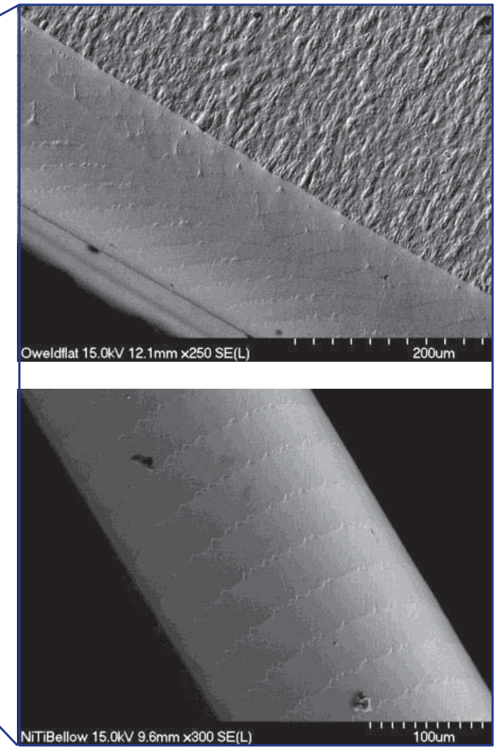

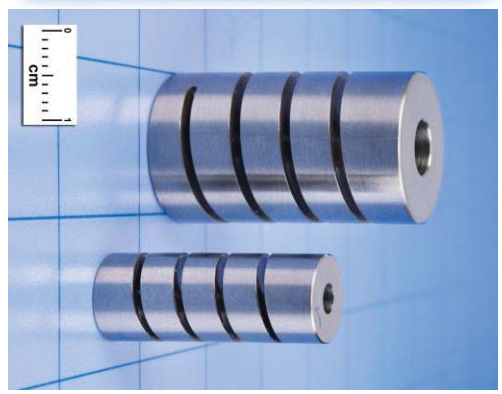

CONSORTIUM FOR THE ADVANCEMENT OF SHAPE MEMORY ALLOY RESEARCH AND TECHNOLOGY

CASMART

Government Academia Industry

Thank You